Rift inheritance controls the switch from thin- to thick-skinned thrusting and basal décollement re-localization at the subduction-to-collision transition

Published Version:
Tavani, S., Granado, P., Corradetti, A., Camanni, G., Vignaroli, G., Manatschal, G., et al. (2021). Rift inheritance controls the switch from thin- to thick-skinned thrusting and basal décollement re-localization at the subduction-to-collision transition. GEOLOGICAL SOCIETY OF AMERICA BULLETIN, 133(9-10), 2157-2170 [10.1130/B35800.1].

Availability:
This version is available at: https://hdl.handle.net/11585/861715 since: 2022-02-20

Published:
DOI: http://doi.org/10.1130/B35800.1

Tavani, Stefano; Granado, Pablo; Corradetti, Amerigo; Camanni, Giovanni; Vignaroli, Gianluca; Manatschal, Gianreto; Mazzoli, Stefano; Muñoz, Josep A.; Parente, Mariano: *Rift inheritance controls the switch from thin- to thick-skinned thrusting and basal décollement re-localization at the subduction-to-collision transition*

GEOLOGICAL SOCIETY OF AMERICA BULLETIN
VOL. 133
ISSN 0016-7606
DOI: 10.1130/B35800.1

Rift inheritance controls the switch from thin- to thick-skinned thrusting and basal décollement re-localization at the subduction-to-collision transition.

Stefano Tavani[1], Pablo Granado[2], Amerigo Corradetti[3], Giovanni Camanni[1], Gianluca Vignaroli[4], Gianreto Manatschal[5], Stefano Mazzoli[6], Josep A. Muñoz[2], Mariano Parente[1]

1 DISTAR, Università degli Studi di Napoli "Federico II", Via Cupa Nuova Cintia 21, 80126, Naples, Italy

2 Institut de Recerca Geomodels, Departament de Dinàmica de la Terra i de l'Oceà, Universitat de Barcelona, C/ Martí i Fraques s/n, 08028, Barcelona, Spain

3 Department of Petroleum Engineering, Texas A&M University at Qatar. Education City, PO Box 23874, Doha, Qatar

4 Dipartimento di Scienze Biologiche, Geologiche e Ambientali, Università degli Studi di Bologna, Via Zamboni 67, 40126, Bologna, Italy

5 IPGS-EOST, Université de Strasbourg-CNRS, 1 Rue Blessig, 67084, Strasbourg, France

6 School of Science and Technology, Geology Division, University of Camerino. Via Gentile III da Varano 27, 62032 Camerino (MC), Italy

Keywords: Thrust tectonics; Structural inheritance, Rifting, Continental collision

ABSTRACT

In accretionary convergent margins, the subduction interface is formed by a lower plate décollement above which sediments are scraped off and incorporated into the accretionary wedge. During subduction, the basal décollement is typically located within or at the base of the sedimentary pile. However, the transition to collision implies the accretion of the lower plate continental crust and deformation of its inherited rifted margin architecture. During this stage, the basal décollement may remain confined to shallow structural levels as during subduction, or re-localize into the lower plate middle-lower crust. Modes and timing of such re-localization are still poorly understood. We present cases from the Zagros, Apennines, Oman, and Taiwan belts, all of them involving a former rifted margin and pointing to a marked influence of inherited rift-related structures on the décollement re-localization. A deep décollement level occurs in the outer sectors of all of these belts, i.e. in the zone involving the proximal domain of pre-orogenic rift systems. Older – and shallower – décollement levels are preserved in the upper and inner zones of the tectonic pile, which include the base of the sedimentary cover of the distal portions of the former rifted margins. We propose that thinning of the ductile middle crust in the necking domains during rifting, and its complete removal in the hyperextended domains, hampered the development of deep-seated décollements during the inception of shortening. Progressive orogenic involvement of the proximal rift domains, where the ductile middle crust was preserved upon rifting, favors its reactivation as a décollement in the frontal portion of the thrust system. Such décollement eventually links to the main subduction interface, favoring underplating and the upward motion of internal metamorphic units, leading to their final emplacement onto the previously developed tectonic stack.

1 INTRODUCTION

Structural reactivation in rifted continental margins during plate convergence is a process of paramount importance in the Wilson cycle (e.g., Wilson, 1966; Jackson, 1980; Cohen, 1982). During convergence, reactivation of structures belonging to the continental margin of the subducting lower plate marks the shift from subduction to collision. This shift typically involves an initial “soft collision” stage, during which the stretched lithosphere of the distal portion of the margin is subducted, and a later “hard collision” stage, which is established upon the inception of poorly-stretched continental lithosphere subduction (e.g., Ballato et al., 2011). The change from soft to hard collision leads to a major tectonic reorganization and commonly results in the reallocation of deformation away from the subduction interface. In accretionary convergent margins, the subduction interface consists of a basal décollement located within or at the base of the lower plate sedimentary pile, the hanging wall of which is scraped off and incorporated into the accretionary wedge (e.g., Nankai: Moore et al., 1990; or Cascadia: MacKay, 1995). With further convergence and inception of the collisional phase, the basal décollement position becomes variable: it can be located either within the lower plate sedimentary cover or within its middle-lower crust (e.g., Oncken et al., 1999; Lacombe and Mouthereau, 2002; Nemčok et al., 2013; Lacombe and Bellahsen, 2016; Pfiffner, 2017). Evidence of the latter case is portrayed by major earthquakes occurring in the crystalline basement in the frontal portions of mountain belts (e.g., the Taiwan 2013 Mw 6.2 Nantou earthquake, Brown et al., 2017; the Zagros 2017 Mw 7.3 Iran-Iraq earthquake, Tavani et al., 2018a), which requires a basal décollement re-localization. Such process apparently contradicts the simple notion that hinterland basement thrusts climb up-section foreland-ward (Fig. 1A), but points out that the inherited crustal rheology across the previous rifted margin may represent a fundamental control in the development of the décollement and in its propagation during plate convergence (e.g., Lacombe and Bellahsen, 2016; Lescoutre and Manatschal, 2020) (Fig. 1B). Consistently, in several mountain belts involving former rifted margins, the distal sedimentary cover is usually detached from its basement to be thrust on top of the proximal and necking domains of the rifted margin. There, thin-skinned thrusting eventually evolves to thick-skinned by the reactivation of deeply rooted faults that deform the overlying thin-skinned system. The Oman Mts. (Tarapoanca et al., 2010), the Apennines (Mazzoli et al., 2014), the European Alps (Schmid et al., 2004), the Taiwan belt (Mouthereau and Lacombe, 2006; Brown et al, 2012; Lacombe and Bellahsen, 2016), and the Zagros belt in the Lurestan region (Vergés et al., 2011) are some well-known examples of this structural evolution. The architecture of these orogenic systems suggests that the re-localization of the basal décollement at deeper structural levels occurs when the necking and proximal domains of the rift system become involved in the collision.

Here we review information from several collisional systems, with an emphasis on the role of inherited rift-related structures, to establish with unprecedented resolution a direct correlation between the structure of collisional orogens and the detailed architecture of precursor rifted margins. Finally, the transition from the first early “soft collision” stage to the later “hard collision” stage is discussed as a possible factor triggering the reorganization of the orogenic wedge, leading to the uplift and exhumation of metamorphic units in the interior of the belt.

2 STRUCTURE OF THE WORK

This work is organized into two main sections: case studies (section 3) and discussion (section 4). The first includes four sub-sections describing each thrust belt and their corresponding reconstructed rifted margins. For each illustrated thrust belt, we present a crustal-scale section and the inferred architecture of the inherited rifted margin. Each case study section is further divided into two parts: the first is a “geological setting”, in which the extant updated literature is reviewed, followed by a “reconstruction of the rifted margin” section, in which the inherited rifted margin architecture is interpreted and discussed in terms of structural domains. In the main discussion, we link the geometry and kinematics of the thrust systems to the structure of the rifted margins, stressing similarities and putting the different belts into an evolutionary order. We first discuss the thrust belts that correspond to the initial stage of décollement re-localization, then we focus on the structure of the more evolved orogens, and eventually infer the driving mechanism for the transition from thin- to thick-skinned thrusting.

3 CASE STUDIES

3.1 The Lurestan region of the Zagros

3.1.1 Geological setting

The Zagros belt developed due to the Cretaceous closure of the Neo-Tethys ocean and the subsequent Cenozoic continental collision between the Arabian and Eurasian plates (e.g., Berberian and King, 1981; Vergés et al., 2011; Mouthereau et al., 2012). The Main Zagros Thrust (MZT) and the Main Recent Fault (MRF) form the still actively deforming suture of the orogenic system (e.g., Talebian and Jackson, 2004), dividing the former Arabian rifted margin to the SW from the Sanandaj-Sirjan block to the NE (Fig. 2) (e.g., Berberian and King, 1981; Ghasemi and Talbot, 2006). To the SW of the suture, the High Zagros Fault (HZF) is a major regional thrust, which hanging wall is mostly composed of the intensely folded and shortened deep-water sedimentary cover of the distal portions of the Arabian rifted margin. The Simply Folded Belt (SFB) in the footwall of the HZF extends to the Mountain Front Flexure (MFF) (Fig. 2A), a major topographic feature controlled by the underlying basement-involved Mountain Front Fault (e.g., Berberian and King, 1981).

The Lurestan Arc is the northwestern salient of the Zagros Mts. (Fig. 2A). It experienced two shortening stages, as recorded by two syn-orogenic foredeep basins of Maastrichtian-to-Eocene and Miocene-to-recent age (Homke et al, 2009; Saura et al., 2015). The older stage involved the northeastern portion of the belt in the hanging wall of the HZF, whereas the younger one mostly involved the SFB (Fig. 2). In the NE area, the tectonic pile exposed in the footwall of the suture includes, from top to bottom (Fig. 2): (i) a thin ophiolite nappe, (ii) the Bisotun-Avalon nappe, and (iii) the Kermanshah-Qulqula nappe (e.g., Vergés et al., 2011). The Bisotun-Avalon nappe is made of sediments of the Upper Triassic to Lower Cretaceous Bisotun-Avalon carbonate platform (Wrobel-Daveau et al., 2010). This carbonate platform formed on top of a crustal block separated from the Arabian margin during the Triassic (Fig. 2D), as marked by the differentiation of the stratigraphic successions of the two domains since that time (Fig. 2B) (Tavani et al., 2018b). The Kermanshah-Qulqula nappe is made up of Lower Jurassic to Upper Cretaceous radiolarites, shales, marls and limestones deposited in the Kermanshah-Qulqula basin (Gharib and De Wever, 2010); this basin was originally interposed between the Arabian margin and the Bisotun-Avalon carbonate platform (Fig. 2D), and partly developed on a exhumed mantle domain (Wrobel-Daveau et al., 2010). This tectonic pile is covered by Paleogene to Miocene continental deposits belonging to the Red Beds Fm. (Koshnaw et al., 2017), which bracket the main activity of the HZF in the Maastrichtian-Paleocene interval. Apart from thin slices of serpentinized peridotites scraped off from the substratum of the radiolarite basin, both the Bisotun-Avalon and Kermanshah-Qulqula nappes are detached from their respective basement and have been telescoped for tens of kilometers along sub-horizontal décollements located within the Triassic (Bisotun-Avalon nappe) and the Lower Jurassic (Kermanshah-Qulqula nappe) successions. Further south, footwall splays of the

HZF occur in the northeastern portion of the SFB (Fig. 3A). These splays are rooted in a Triassic décollement level, have displacements in the order of some kilometers, and are roughly coeval with the HZF, since their associated folds are truncated by the HZF (Tavani et al., 2018a).

The SFB is characterized by low-displacement thrusts, by a mixed thin- and thick-skinned style of deformation, and by a remarkably different Mesozoic sedimentary succession with respect to that exposed in the hanging wall of the HZF. In detail, the Arabian margin sedimentary succession in the Lurestan Arc includes 6-8 km of Mesozoic-Cenozoic clastic and carbonate rocks (Fig. 2B) overlying *ca.* 4 km of Paleozoic units (Hessami et al., 2001; Vergés et al., 2011).

Apart from the splays of the HZF (Fig. 3A), the proximal domain of the Arabian margin was deformed in a piggy-back sequence since the Miocene (Barber et al., 2018). The basement-cover interface of the SFB is recognized as a regional mechanical weakness, which promoted partial decoupling between the sedimentary cover and the crystalline basement (Vergés et al., 2011; Tavani et al., 2018a). In detail, low-displacement reverse basement faults ramp-up to join the basement-cover interface, above which the sedimentary cover is mostly shortened by folding (Fig. 2C). Steeply-dipping basement thrusts are rooted into a mid-crustal décollement at about 20-25 km depth (e.g., Vergés et al., 2011), and many of them are interpreted as inverted extensional faults (Tavani et al., 2018a). The occurrence of the mid-crustal ductile décollement level is also evidenced by a seismic gap occurring between 20 and 30 km depth (e.g., Talebian and Jackson, 2004; Tavani et al., 2020). The Mountain Front Fault is a moderate- to gently-dipping active thrust at the tip of the mid-crustal décollement, with a displacement in the order of 10 km (Vergés et al., 2011; Tavani et al., 2018a). The development of the Mountain Front Fault occurred in a very recent stage of the thrust belt evolution, approximately <3 Ma (Tavani et al., 2020), thus representing the youngest feature of the belt. With the exception of this fault, displacement along basement reverse faults is rather limited.

3.1.2 Reconstruction of the rifted margin

The Arabian margin involved in the Zagros Belt underwent two-stage rifting, during the Permian-Triassic and the Early-Middle Jurassic intervals (Tavani et al., 2018b). However, the first stage poorly affected the Lurestan region and the tectono-stratigraphic architecture of the margin mostly results from the Early-Middle Jurassic extensional tectonics, coeval with the development of the Kermanshah-Qulqula basin (Tavani et al., 2018b). During this extensional phase, large areas evolved from shallow to deep-water depositional environments (Figs. 2B, 3A) (e.g., Barrier and Vrielynck, 2008), with largely underfilled Middle and Late Jurassic basins where deep-water conditions persisted until the Late Cretaceous onset of convergence. Middle to Upper Jurassic rocks are poorly exposed in the SFB, hence a clearer marker of the drowned Jurassic tracts is provided by the extensively exposed Lower Cretaceous facies, which are here used to infer the limits between the different domains of the rifted margin.

In detail, three domains can be recognized (Fig. 2B). To the SW, shallow-water carbonate sedimentation spans from the Permian until the Late Cretaceous (Fig. 2A, B). This large area did not experience remarkable crustal thinning and corresponds to the unstretched Arabian Plate (Fig. 2D). The central part of the study area corresponds to the proximal domain of the Arabian Jurassic rifted margin, which records crustal stretching and drowning. This is witnessed by the deep-water Lower Cretaceous Garau Fm., which is made up of limestones, marls, and shales (Jassim and Goff, 2006). Radiolarian-rich beds in its lower portion are well known (Fig. 3B) and testify for a paleobathymetry near the carbonate compensation depth (CCD) and basin starvation. Here we firstly report that in the northernmost area, the Garau Fm. also includes m-thick radiolarites (Fig. 3C), thus representing even deeper facies (below the CCD), transitional between the typical radiolarian-rich Garau Fm. and the radiolarites of the Kermanshah-Qulqula basin. In our interpretation, this transitional facies is indicative of an area that was part of the necking domain of the Jurassic rift, transitional between the stretched proximal domain and the hyperextended Kermanshah-Qulqula radiolarite basin, in which local mantle exhumation is reported (Wrobel-Daveau et al., 2010). The width of the Kermanshah-Qulqula radiolarite basin and of the Bisotun-Avalon extensional ribbon are from Verges et al. (2011).

3.2 The southern Apennines

3.2.1 Geological setting

The Late Cretaceous to Quaternary Apennines belt developed within the framework of Africa-Eurasia plate convergence (e.g., Dewey et al., 1989; Doglioni, 1991; Faccenna et al., 2014). In this subduction-to-collision system, Eurasia represented the overriding plate, whereas the downgoing plate included the Jurassic to Early Cretaceous Alpine Tethys ocean and its southern rifted margin, i.e. the Adria promontory of Africa. Remnants of the overriding plate are extensively outcropping in southernmost peninsular Italy and in northern Sicily, in the so-called Calabria-Peloritani Arc (Somma et al., 2005, and references therein). These continental crust units overthrust ophiolitic rocks (Liguride complex; Ogniben, 1969), exposed along the tectonic suture. In the southern Apennines, convergence was characterized by a roughly E- to NE-ward migration of the thrust front and the related foreland basin (e.g., Menardi Noguera and Rea, 2000; Patacca and Scandone, 2007) and by the progressive tectonic incorporation of the Mesozoic-Tertiary domains established on the Adria promontory of Africa during the Late Triassic to Early Jurassic rifting stage. In summary, Triassic to Jurassic divergence between Gondwana and Eurasia led to the opening of the Alpine Tethys, of which Adria formed part of the SE rifted margin. There, a suite of horst and graben/half-graben structures formed upon rifting, in which carbonate platforms and pelagic basins developed. In the southern Apennines, these Mesozoic domains are, from west to east (Fig. 4D): the Apennine carbonate platform, the Lagonegro pelagic basin, and the Apulian carbonate platform (Ogniben, 1969; D’Argenio et al., 1975; Patacca and Scandone, 2007; Cosentino et al., 2010; Santantonio and Carminati, 2011).

During the Eurasia-Adria Cenozoic convergence, deep-water sediments and slices of ophiolites were scraped off from the downgoing Tethys oceanic plate and accreted to form the Liguride complex (Ogniben, 1969; Knott, 1987). During the middle Miocene, this accretionary complex was thrust eastward for tens of kilometers and placed on top of the Apennine Platform and its Miocene syn-orogenic cover (e.g., Roure et al., 1991; Menardi Noguera and Rea, 2000; Scrocca, 2010). To date, only a few exposures of slope and/or basin facies located to the west of the Apennine Platform are reported in the area (Capri Island, ISPRA 2014; Curzi et al., 2020), indicating that the entire necking and hyperextended domains between the Apennine Platform and the Liguride basin has been overthrust by the Liguride complex. During the middle to late Miocene, the tectonic pile was detached along a basal décollement placed at the base of the sedimentary cover of the Apennine platform and was thrust NE-ward on top of the Lagonegro basin units. Finally, during the Pliocene, the sedimentary cover of the Lagonegro basin was also detached from its pre-Mesozoic basement and placed on top of the Apulian Platform (Roure et al., 1991; Menardi Noguera and Rea, 2000). The latter is presently buried below the thin-skinned thrust belt and rises to the NE, being exposed in the foreland region. The décollement between the allochthonous units and the buried Apulian Platform unit is marked by a fluid-saturated, clay-rich mélange zone of variable thickness, reaching up to ca. 1500 m (Mazzoli et al., 2001; Fig. 4). The above described thin-skinned tectonic pile has been re-deformed by subsequent late Pliocene to early Pleistocene shortening, controlled by steeply-dipping reverse faults rooted in the Apulian Platform basement (Mazzoli et al., 2014) (Fig. 4C). Immediately to the SW of these faults, seismic data indicate the occurrence of a slope domain between the Apulian Platform and the Lagonegro basin (Menardi Noguera and Rea, 2000). This slope domain is currently in the footwall to the Lagonegro basin basal thrust, which in turn is to the footwall of the Apennine Platform basal thrust. Importantly, the Moho across this area rises up from 32-34 km to the NE to 26-28 km to the SW (Menardi Noguera and Rea, 2000; Di Bucci et al., 2006; Mazzoli et al., 2014). It is noteworthy that thick-skinned thrusting has not developed in the Apennine Platform, which was originally interposed between two areas of hyper-extended crust. Deeply rooted thrusts linked to a deep crustal décollement have developed only when a significant portion of the proximal domain of the Apulian platform has been involved in the orogenic pile.

3.2.2 Reconstruction of the rifted margin

Triassic to Early Jurassic extension in the Adria crustal block led to the formation of a rifted margin made of a suite of carbonate platforms and pelagic basins. Our reconstruction of the margin is shown in Figure 4D. The Lagonegro basin is here interpreted as a hyperextended domain due to the occurrence of deep-water radiolarites deposited below the CCD in its central parts (in which the whole Jurassic column consists of 70-80 m of radiolarian cherts and siliceous argillites; Mazzoli et al., 2001, and references therein), with a commonly inferred width of nearly 150 km (Menardi Noguera and Rea, 2000; Scrocca et al., 2005). On the other hand, the pre-orogenic width of the Apennine carbonate platform is estimated to be nearly 60 km (Menardi Noguera and Rea, 2000; Mazzoli et al., 2014); this value is slightly underestimated, since the transition between the Apennine carbonate platform and the basin located to the SW is generally not included in cross sections. In this sense, as exposures of slope and/or basinal facies occur a few tens of km to the SW of the coastline (e.g., Capri Island, ISPRA 2014), the maximum original width for the Apennine carbonate platform (including the surrounding slope domains) should not exceed 100 km.

An important feature for the rifted margin reconstruction is the step in the Moho observed along the SW portion of the regional cross section (Fig. 4C). The Moho step has been previously interpreted as associated with a SW-dipping reverse fault affecting the upper mantle and the crust (Menardi Noguera and Rea, 2000). However, we propose a different interpretation coherent with the main message of this work and contractional slip transfer considerations. The step is here interpreted as a NE-dipping lower crust extensional shear zone related to Mesozoic crustal thinning. Our interpretation is strongly supported by the two following observations: (i) the Moho step is placed exactly underneath the slope domain interposed between the Apulian shallow-water carbonate platform and the Lagonegro deep-water basin, i.e. exactly where crustal extension is to be expected; and (ii) in agreement with the transition between the two different depositional environments, the pre-orogenic crustal thickness reduces from 30 km to the NE (Apulian Platform cover plus the middle and lower crust) down to less than 20 km to the SW (Lagonegro basin cover plus the middle and lower crust); such a crustal thinning requires significant extension in the area. Within this framework, the Moho step would be placed within or immediately to the NE of the boundary between the former necking and proximal domains (Fig. 4D). No information instead is available to define the position and width of the necking domains that bounded the Apennine Platform to the NE and SW. Similarly, the width of the hyperextended domain between the Neo Tethys and the Apennine Platform shown in figure 4C is highly speculative.

3.3 Oman

3.3.1 Geological setting

The Oman mountain belt (also known as Al-Hajar mountains) developed following the Late Cretaceous closure of the Neo-Tethys ocean between the Arabian and Eurasian plates, and by subsequent shortening during the Cenozoic (Glennie et al., 1973; Tarapoanca et al., 2010; Hansman et al., 2017). Ocean closure was initiated by intra-oceanic NE-directed subduction (Robertson and Searle, 1990; Jolivet et al., 2016), followed by the generation of the Semail ophiolites in a supra-subduction environment at 96-95 Ma (e.g., Robertson and Searle, 1990; Rioux et al., 2012). The obducted Semail ophiolites occupy the uppermost portion of the Oman tectonic pile (Fig. 5). The thin metamorphic sole at the base of the Semail ophiolite peridotite records amphibolite facies metamorphism at 95-92 Ma (i.e. 54-46 km depth, Searle and Cox, 2002). Obduction initiated at 95-93 Ma (Hacker, 1994), when the Semail ophiolites were thrust over the various domains of the distal portion of the former Arabian rifted margin. The highly deformed and partly dismembered remnants of the Arabian margin are presently sandwiched between the Semail ophiolites and the Arabian shelf, which includes the stable continent and the proximal domain of the rift. The northeastern portion of the Arabian shelf was involved in the subduction, as recorded by blueschist to eclogite facies metamorphic rocks exposed at the Saih Hatat tectonic window (SH in Fig. 5A) (Chemenda et al., 1996; Breton et al., 2004). During convergence, the sedimentary cover of the distal domains of the Arabian margin was progressively detached from its basement, incorporated into the tectonic wedge, and thrust on top of the proximal domain of the Arabian rifted margin. During the foreland-ward migration of the allochthonous wedge, the Arabian foreland underwent SW-migrating flexural bending with uplift and erosion of the rifted margin, as witnessed by the development of a Turonian unconformity (Boote et al., 1990; Cooper et al., 2014) dating the onset of deformation related to convergence in the Arabian shelf. The wedge emplacement onto this Late Cretaceous foredeep ended by the Campanian (Warburton et al., 1990), almost coevally with the eclogite-facies metamorphism recorded in the Saih Hatat rocks at around 79 Ma (Warren et al., 2003). Stable shelf conditions alternated with emersion periods during the early Maastrichtian to Eocene time interval, leading to the sedimentation of an unconformable post-kinematic sequence (Post-Nappe in figure 5) covering the Cretaceous wedge to the NE and progressively becoming conformable over the foredeep sediments to the SW.

During the Cenozoic, a second shortening phase occurred, responsible for the deformation of the Upper Cretaceous to Cenozoic Post-Nappe package (Corradetti et al., 2020) and for the final uplift and doming of the Jabal Akhdar and Saih Hatat structural culminations (Mount et al., 1998; Breton et al., 2004; Cooper et al., 2014; Hansman et al., 2017). Late deformation is well constrained by thermochronological data (Mount et al., 1998; Saddiqi et al., 2006; Tarapoanca et al., 2010; Hansman et al., 2017; Corradetti et al., 2020) and absolute radiometric dating of veins from tectonic windows and surrounding tectonic units (Grobe et al., 2018; Hansman et al., 2018). Despite the large debate on the timing and modes of exhumation of the Oman mountains, available data point toward a rapid exhumation starting from the early Eocene, at 45-40 Ma, (Tarapoanca et al., 2010; Jacobs et al., 2015; Hansman et al., 2017), and a later reactivation at 20-15 Ma (Jacobs et al., 2015; Corradetti et al., 2020). Eocene uplift and unroofing relate to a major shortening event that affected the whole nappe edifice, triggering flexuring of the lower plate (e.g., Homewood et al., 1986) and development of a new foredeep (Tarapoanca et al., 2010; Corradetti et al., 2020). Such shortening event is associated with thick-skinned thrusting, most-likely resulting from positive inversion of pre-existing basement faults inherited from the Permian-Triassic extensional phase (Boote et al., 1990; Tarapoanca et al., 2010; Hansman et al., 2017). Notably, in the area crossed by our section no evidence of thick-skinned tectonics during the Cretaceous stage has been documented so far for the Arabian shelf.

3.3.2 Reconstruction of the rifted margin

The Arabian rifted margin in the Oman region formed during the Permo-Triassic magma-rich rifting (e.g., Robertson and Searle, 1990). The different paleogeographic domains of the margins are the Arabian Shelf to the SW, and the Hawasina basin to the NE, the latter including the Sumeini slope, and the Hamrat Duru and Umar deep-water basins separated by remnants of platform carbonates such as the Kawr Group (Fig. 5D) (Béchennec et al., 1988; Rabu et al., 1993). Accordingly, we here interpret these paleogeographic domains in terms of structures of a rifted margin. In detail, the reconstruction of the Arabian margin includes, from SW to NE: (i) the proximal domain (NE portion of the Arabian shelf) characterized by a Neo-Proterozoic to Cretaceous sedimentary pile exposed in the Jabal Akhdar and the Saih Hatat culminations and in the Musandam peninsula (JA, SH, and MU in figure 5A), where shallow water conditions persisted during the Mesozoic; (ii) the Sumeini slope, where deep water facies (including > 10 m thick packages of radiolarites) are intercalated with distal calcarenites during the Permian-Cretaceous time span. We infer that the occurrence of these thick packages of radiolarites is indicative of deep-water conditions (close to the CCD depth) and basin starvation, which we correlate with the necking domain. Thus, the NE portion of the Sumeini slope in our reconstruction coincides with the necking domain; (iii) the distal portion of the margin, mostly made by the deep-water sediments resting on top of Permian-Triassic syn-rift volcanic rocks. In detail, the latter domain is divided in two basins: the Hamrat Duru and Umar basins, separated by a narrow domain (Kawr), in which shallow-water carbonate platform conditions persisted at least during the Triassic rifting, constituting an elevated feature (horst) throughout the Jurassic-Cretaceous times (Béchennec et al., 1988; Rabu et al., 1993). The occurrence of the Kawr carbonate platform within the distal portion of the margin mimics the structure of the Bisotun-Avalon carbonate platform of the Zagros and of the Apennine Platform of the southern Apennines. In agreement, we suggest that the Kawr carbonate platform represents a continental ribbon (sensu Péron-Pinvidic and Manatschal 2010) (Fig. 5D). The preserved geological record of this ribbon is not sufficiently detailed to allow estimating the position of the necking domains surrounding it and, in agreement, these necking domains are not indicated. More generally, the width of the different domains reported in figure 5D remain speculative (albeit in full agreement with their typical width documented worldwide; Chenin et al., 2017), as the far-travelled and highly re-imbricated nature of the thrust sheets of the Oman belt prevents accurate reconstructions. Indeed, only the cumulative width of the entire Hawasina basin is generally reconstructed, being at least 400 km-wide (Béchennec et al., 1988; Cooper, 1988).

3.4 The Taiwan mountain belt

3.4.1 Geological setting

The Taiwan mountain belt is forming since the late Miocene (6.5 Ma, Lin et al., 2003) as a result of the oblique collision between the nearly NE-SW oriented Eurasian rifted margin and the approximately N-S trending Luzon volcanic arc on the Philippine Sea Plate (e.g., Teng, 1990; Sibuet and Hsu, 2004; Huang et al., 2006; Byrne et al., 2011; Brown et al., 2012) (Fig. 6). In more detail, the Eurasian rifted margin formed during the opening of the South China Sea during the Oligocene–Miocene, whereas collision took place after an initial phase of E-directed subduction of the South China Sea oceanic lithosphere below the Philippine Sea plate, which started about 15 Ma ago and is still active south of Taiwan (e.g., Huang et al., 2006). From its more internal (i.e., eastern) to its more external (i.e., western) parts, the Taiwan mountain belt comprises five fault-bounded domains: the Coastal Range, the Central Range, the Hsuehshan Range, the Western Foothills, and the Coastal Plain (Fig. 6A,C). The Coastal Range is made up of volcanic rocks of the Luzon arc and sediments deposited within intra-arc basins, and it is juxtaposed against the Central Range along the Longitudinal Valley Fault (LVF, Fig. 6), which is thought to represent the plate boundary within the collision zone (e.g., Shyu et al., 2008). The Central Range comprises from west to east (Fig. 6C): (i) the Lushan slate belt, made of syn- to post-rift Eocene to Miocene sediments (Clark et al., 1993; Beyssac et al., 2007; Simoes et al., 2007; Brown et al., 2012), which underwent low-grade syn-orogenic metamorphism (Beyssac et al., 2007); (ii) the Tananao Complex, a greenschist facies metamorphic complex (e.g., Chen et al., 2017) made of Mesozoic pre-rift basement rocks of the Eurasian rifted margin (i.e. marbles and schists), and (iii) the Yuli belt, the remnants of a Miocene accretionary prism with exotic blueschist blocks (e.g., Chen et al., 2017) that reached high-pressure metamorphic conditions during subduction (Keyser et al., 2016). The Tananao Complex is thrust over the Lushan belt along the Chinma thrust. Exhumation of the Tananao Complex along the Chinma thrust took place during the early to late Pleistocene (Dorsey, 1987; Lee et al., 2006; Brown et al., 2012) and some authors have linked its development to underplating and nappe stacking processes (e.g., Simoes et al., 2007; Molli and Malavieille, 2011) (Fig. 6C). The Central Range is juxtaposed against the Hsuehshan Range across the Lishan Fault in the north (Clark et al., 1993; Brown et al., 2012) and against the Western Foothills across the Chaochou Fault in the south (Mouthereau et al., 2002; Tang et al., 2011, Fig. 6A). The Hsuehshan Range comprises variably metamorphosed Eocene and Oligocene clastics (Beyssac et al., 2007; Simoes et al., 2012) that were deposited within the Hsuehshan basin on the Eurasian rifted margin (Teng and Lin, 2004; Huang et al., 2006; Brown et al., 2012) (Fig. 6C,D). High-temperature metamorphism of this portion of the belt, that represents an outlier in the eastward-increasing metamorphic trend, has been interpreted as associated with the rifting stage, rather than with mountain building (Beyssac et al., 2007). The Western Foothills consist of imbricated Eocene to Miocene syn- to post-rift sediments and younger syn-orogenic sediments (Lacombe et al., 1999; Yue et al., 2005; Brown et al., 2012) (Fig. 6C). Finally, the Coastal Plain is made up of weakly deformed Pliocene to Holocene syn-orogenic sediments of the foreland basin.

The Taiwan mountain belt displays a hybrid, thick- and thin-skinned, structural style. The basal décollement of the Western Foothills is located nearly at the base of the syn-orogenic sediments. Conversely, in the more internal domains, rocks of the pre-rift basement are involved in the deformation and crop out in the Tananao Complex (Fig. 6C). Surface geology (Clark et al., 1993; Mouthereau et al., 2002; Brown et al., 2012; 2017) and the shallowing of high P-wave velocities taking place along deeply rooted clusters of earthquake hypocenters in the interior of the mountain belt (Gourley et al., 2007; Wu et al., 2007; Kuo-Chen et al., 2012; Brown et al., 2017), indicate that basement is uplifted along steeply dipping faults that penetrate into the middle crust and formed as a result of the inversion of pre-existing extensional faults (Mouthereau and Lacombe, 2006; Brown et al., 2012; 2017; Lacombe and Bellahsen 2016) (Fig. 6D). For example, the development of the Hsuehshan Range is associated with the inversion of the Hsuehshan basin due to the reactivation of its bounding faults (i.e., the Shuilikeng and the Lishan faults; Brown et al., 2017; Fig. 6C,D).

Importantly, the Eurasian rifted margin underwent at least two major phases of deformation during convergence that led to the development of the Taiwan mountain belt (Brown et al., 2012). With the arrival of the leading edge (i.e., distal part) of the margin at the subduction zone, a first phase of thin-skinned deformation was responsible for detaching (and westward translation) of the syn- to post-rift sediments from their pre-rift basement (i.e., the current Lushan belt; Brown et al, 2012); the Tili thrust represented the leading thrust during this initial thin-skinned deformation phase. Remnants of this first thrust system can be currently found in the Taiwan mountain belt as a folded and faulted thrust fault cropping out in the Hsuehshan Range and in the Lushan slate belt, and inferred also in the eroded portion of the Tananao complex (Fig. 6D). Once the relatively poorly extended proximal domain of the rifted margin reached the subduction zone as convergence proceeded, shortening was mostly accommodated by thick-skinned inversion of pre-existing extensional faults and extensive basement uplift as described above (Mouthereau and Lacombe, 2006; Brown et al., 2012; 2017) (Fig. 6D).

3.4.2 Reconstruction of the rifted margin

Prior to collision in Eocene times, the Eurasian margin had the structure of a hyperextended margin (Brown et al., 2012; McIntosh et al., 2013) (Fig. 6D). In the cross-section of Figure 6C, the thinned crust of the hyperextended domain is not present as resulting from the subduction of the entire distal domain (e.g., McIntosh et al., 2005). However, the obliquity between the rifted margin and the thrust belt, and the preservation of the former in the foreland of the southern portion of the Taiwan belt, allows setting the approximate boundaries between the different rift domains. In detail, in figure 6D we show a slightly modified version of the reconstruction by Brown et al. (2012). In particular, albeit with some uncertainty, the necking domain in the cross-section of Figure 6C can be reasonably placed some tens of km to the east of the suture, coherently with the eastward thinning of the crust which occurs in the subducted plate. In fact, despite the remarkable deformation, the crustal thickness underneath the Hsuehshan and Central ranges (particularly the occurrence of a thick basement overlying the ductile crust), indicates that these areas were forming part of the proximal domain.

4 DISCUSSION

This discussion is organized in three sub-sections. Firstly, we recall the structure of the four illustrated rifted margins, stressing their architecture and the recognition of different structural domains. Then, we discuss the process of décollement re-localization and, finally, we discuss our findings in the context of the role of structural inheritance in mountain building processes.

4.1 Recognition of inherited rifted margins

4.1.1 Lurestan region of the Zagros

The architecture of the former Arabian rifted margin in the Lurestan is nowadays well understood (e.g., Wrobel-Daveau et al., 2010; Vergés, et al., 2011; Saura et al., 2015; Fig. 2D), and archetypal domains of hyperextended magma-poor rifted margins (e.g., Whitmarsh et a., 2001; Lavier and Manatschal, 2006; Péron-Pinvidic and Manatschal 2009) have recently been recognized in this area. To the NE, the Bisotun-Avalon carbonate platform marks the occurrence of a former extensional ribbon of continental crust (*sensu* Lister et al. 1986). In addition, the presence of radiolarites, indicating paleo-water depths below the CCD (De Wever et al., 1994), and the occurrence of serpentinized peridotites underlying them (Wrobel-Daveau et al., 2010) reveal that the Kermanshah-Qulqula basin represents a hyperextended (i.e. a domain in which the continental crust was thinned down to less than 10 km; Péron-Pinvidic and Manatschal, 2009) to exhumed mantle domain. The necking domain of the Jurassic margin, i.e. the thinned and faulted part separating the weakly extended crust of the proximal domain from the hyperextended domain, may be placed in the NE portion of the Arabian margin (Fig. 2), coherently with the fact that the post-rift

Garau Fm. there includes meter-thick radiolarites (Figs. 2,3) pointing to the proximity of the CCD. To the SW, the area labeled as “Arabian Plate” is the region devoid of any significant crustal stretching.

4.1.2 Southern Apennines

The telescoped Adria rifted margin presently incorporated in the southern Apennines is also well constrained (e.g., D’Argenio et al., 1975; Patacca and Scandone, 2007; Cosentino et al, 2010). In this area, the southern margin of the Alpine Tethys has been defined as a Triassic to Early Jurassic magma-poor rifted margin (e.g., Mohn et al., 2012). Deep water radiolarites occur in the central portion of the Lagonegro basin (e.g., Mazzoli et al., 2001) and the observed thinning of the crust down to ~20 km at the transition with the Apulian Platform (Fig. 4C) allows interpreting at least the central part of the Lagonegro basin as a hyperextended domain. The Apennine Platform, in between the Lagonegro basin to the east and the Alpine Tethys to the west, can be regarded as an extensional ribbon, similar to the Bisotun-Avalon carbonate platform of the Lurestan area. The former necking domain of the western rifted margin of Adria can be located along the eastern margin of the Lagonegro basin, immediately to the SW of the Moho step (Fig. 4C); within this framework the Apulian Platform would represent the proximal rift domain.

4.1.3 Oman

The former Arabian rifted margin in the Oman Mts. slightly differs from that of the Lurestan, in terms of both timing and magma supply. The timing of rifting is Permian-Triassic, as recorded by the Triassic deep-water sedimentary record (e.g., Rabu et al., 1993). Furthermore, the abundant Permian volcanites included in various sedimentary successions of the Hawasina basin (e.g., Robertson and Searle, 1990) point to significant magmatic input. Apart from these differences, the shallow-water carbonates of the Kawr domain, between the deep-water Hamrat Duru and Umar domains, were most likely also deposited on an extensional ribbon. Radiolarites belonging to the Hamrat Duru and Umar domains suggest a paleodepth close to the CCD and a remarkable crustal thinning for these domains. Consistently, the crustal-scale cross-section in Figure 5C shows that the pre-orogenic crust at the Sumeini slope to Arabian shelf transition, i.e. in the thicker portion of the Hawasina basin, should have been nearly 20 km thick. Accordingly, we infer hyper-extension in the Hamrat Duru domain, which was placed in a more distal position with respect to the 20 km thick crust of the Sumeini slope. The substratum of the Umar sub-basin is instead interpreted as made of both hyperextended continental crust and oceanic crust.

4.1.4 Taiwan

The rifted margin deformed in the Taiwan belt is the least constrained one (Fig. 6). Rifting is Eocene in age (Brown et al., 2012; McIntosh et al., 2013) and no record for extensional ribbon occurs there. The margin consisted of three sectors matching the proximal, necking and hyperextended domains; however, neither the basement nor the respective sedimentary covers of the latter two domains are exposed. On the other hand, the geometry of these extensional domains as well as the approximate location of their boundaries, can be proposed by taking advantage of the obliquity between the rifted margin and the thrust belt (i.e. the former proximal domain of the margin is preserved on the active foreland at the southern portion of the Taiwan belt; e.g., Brown et al., 2012).

4.2 Décollement re-localization at the transition from subduction to collision

After rifted margin development and during the subsequent plate convergence, the distal parts of the rifted margin arrives to the subduction zone once the attached oceanic crust has been consumed during subduction. At this stage, the basal décollement propagates from the base of the ophiolitic sequence into the base of (or within) the rifted margin sedimentary cover. The involvement of continental extensional ribbons seems not to produce any remarkable effect on the thin-skinned thrust system: examples illustrated above indicate that the basal décollement remains confined to the sedimentary cover by shearing off the structural highs. When the hyperextended domain of the lower plate (i.e. the Lagonegro basin in the Apennines; the Kermanshah-Qulqula basin in Lurestan; and the Hamrat Duru sub-basin in Oman) arrives at the trench, shortening is still accommodated by thin-skinned thrusting. This is shown by the Lagonegro basal thrust, the High Zagros Fault, and the Hawasina basal thrust, which detached and telescoped the sedimentary succession of the distal portion of the rifted margin on top of its proximal domain.

As collision evolves, slightly different evolutions can be defined based on the examples above. In the Lurestan, the thin-skinned basal décollement propagated from the hyperextended domain into the necking domain across weak stratigraphic levels. Further shortening and convergence (re-)activated the inherited basement faults of the necking and proximal domains. The first stage of this thick-skinned deformation is characterized by limited shortening accommodated by inversion tectonics (Granado and Ruh, 2019; Tavani et al., 2020). In the latest stage of deformation, the seismically active low-angle Lurestan Mountain Front Fault developed, with a cumulative displacement of nearly 10 km. The activity of this fault testifies the presence of an efficient and laterally continuous mid-crustal décollement along which large displacement is accumulated. In the central portion of the Oman Mountains, Late Cretaceous convergence ended with the emplacement of the obducted Semail supra-subduction ophiolites and the distal margin sedimentary cover onto the Arabian shelf, besides locking of major thrusts. The Arabian shelf includes both the stable Arabian plate and the proximal domain of its margin, and no evidence for any remarkable Cretaceous thick-skinned tectonics can be found in the area crossed by our section. In this portion of the tectonic pile, the development of major basement thrusts, and related development of the Jabal Akhdar structural culmination are attributed to the second (i.e. Cenozoic) shortening pulse (Hansman et al., 2017). In the frontal portion of the Oman belt, secondary décollement levels developed within the sedimentary cover of the Arabian shelf (Corradetti et al., 2020); however, these décollement levels probably emanate from deeply rooted thrusts and do not connect with the Hawasina basal thrust. Such situation resembles the structural style observed in the southern Apennines, where no remarkable décollement levels occur in the sedimentary cover of the Apulian platform. Indeed, after the emplacement of the thin-skinned tectonic wedge (i.e. including the Liguride, the Apennine Platform, and the Lagonegro basin units) onto the Apulian Platform (i.e.

the proximal domain of the margin), the basal décollement directly re-localized into the middle-lower crust. Further shortening has been transferred to the proximal domain by the development of deep-seated, basement-involving thrusts.

Apart from the different propagation of the thin-skinned basal décollement in the proximal domain of the Lurestan, Apennine and Oman belts, their common history shows that the involvement of the mid-crustal décollement initiates in the proximal domain once the necking domain enters the subduction channel, marking the transition from soft to hard collision. The switch in shortening style is therefore mainly controlled by the crustal thickness and rheology inherited from the rifted margin. In detail, the inherited rheology corresponds to the transition from thinned crust in the necking domain to normal thickness crust in the proximal domain (Fig. 1B). During shortening of the hyperextended domain, the coupled crust and upper mantle are characterized by a dominating brittle-frictional rheology. During this stage, the main reactivation-prone mechanical weakness is the basement-cover interface, often represented by an exhumation fault soled along hydrated crust or serpentinized mantle (e.g., Sutra et al., 2013; Lescoutre and Manatschal, 2020). With the arrival of the necking domain in the subduction zone (Fig. 7), the weak mid crustal level, absent in the hyperextended crust as a result of rifting and crustal thinning (Fig. 7A-C), may localize forelandward-directed simple shear (Fig. 7D-E) and constitute a large interconnected décollement linked with the main subduction interface.

Once activated, the mid-crustal décollement propagates forelandward across the preserved middle crust ductile level of the proximal domain (as seen in Oman, Lurestan, and Apennine belts), but also hinterland-ward. The hinterland-ward propagation of the mid-crustal ductile level is also ensured by the increased metamorphic conditions within the subducting thinned continental crust, which allows ductile deformation to occur in the former hyperextended domain of the rift (Fig. 7D-E). At this stage, the subduction interface re-localizes at a deeper structural level, allowing for basal accretion and crustal stacking (as seen in Taiwan), which in turn allows for the internal reorganization of the orogenic wedge by the exhumation of hinterland metamorphic units (Fig. 7D).

Notably, thin-skinned thrusting observed in the Kawr (Oman), Bisotun-Avalon (Lurestan), and Apennine Platform (Apennines) extensional ribbons, indicates that their sedimentary cover has been detached from the basement and this basement has not been later involved in thrusting. Therefore, although we have inferred a pre-orogenic ductile middle crust for these extensional ribbons, its activation as a basal décollement - if any - must have been limited (e.g. some low-displacement upper crustal duplexes linking upward with the basement-cover interface and soling down into the middle crust; however, these structures have not been found in any of those three belts). But why the ductile crust within these extensional ribbons does not significantly activate with their arrival at the subduction zone? We can just speculate about two hypotheses: (1) The cross-sectional width of the Bisotun-Avalon and Apennine Platform extensional ribbons, excluding the necking domains bounding them, is largely below 100 km (Figs. 2D, 4D). Accordingly, a few tens of kilometers tract of thick ductile middle crust could be not enough to nucleate a regional ductile décollement level. (2) The ductile crust underneath extensional ribbons could be actually thinner and less interconnected with respect to a “normal” proximal domain. In the end, the extensional ribbons illustrated in this work do not show evidence of thick-skinned thrusting and mid-crustal décollement level activation, because either these blocks are not large enough or their ductile crust is not thick and interconnected enough, or a combination of both.

4.3 Rift-inheritances and thrust tectonics

Since the 80’s, normal faults reactivated with a reverse kinematics have been documented worldwide (e.g., Williams et al., 1989; Nemčok et al., 1995; Marshak et al., 2000; Zanchi et al., 2006; Carrera et al., 2006). This observation has shaped the concepts of inversion tectonics (e.g., Glennie and Boegner, 1981; Cohen, 1982; Cooper et al., 1989) and structural inheritances (e.g., Butler and Mazzoli, 2006, and references therein). It is largely demonstrated that the map outline of orogens partly retraces the shape of the inherited rift systems (e.g., Macedo and Marshak, 1999; Lescoutre and Manatschal, 2020). This overlap is due to various reasons: (i) the reactivation of basin-bounding faults (e.g., Carrera et al., 2006); (ii) the rift architecture control on the lateral extent of sedimentary units that can act as decoupling levels (e.g., Bellahsen et al., 2012; Muñoz et al., 2013); and (iii) the variable thickness of the ductile crust in the different inherited extensional domains that allows/prevents the development of a mid-crustal décollement level (e.g., Lacombe and Bellahsen, 2016; Tavani et al., 2020). The four collisional systems presented in this study, despite the differences and simplifications we have introduced, have allowed us to further expand the last concept of rift-related crustal rheological inheritances. The interaction between evolving rheological properties of the lithosphere and orogen growth has been quantitatively demonstrated by numerical models (e.g., Jamieson and Beaumont, 2013), which have also improved our understanding of how inherited crustal composition, and the resultant variation of crustal strength, may control orogenic processes (e.g., Jammes et al., 2014). In line with these numerical results, we have demonstrated the correspondence between the evolution of collisional systems, from thin-skinned to thick-skinned and eventually to underplating and crustal stacking, and the rheology of the extensional domain subducted at each stage of plate convergence.

5 CONCLUSIONS

Our review of geological data from four orogenic systems reactivating their former rifted margins shows a close link between the evolution of the orogenic system and the inherited crustal architecture and related rheology. In all the reviewed systems, the first stage of collision corresponds to the activation of a thin-skinned décollement level, along which the sedimentary cover of the distal portions of the former rifted margin has been detached from its basement and has been placed onto the former proximal domain. This level forms in the previously thinned domain of the margin, where syn-rift coupling between the brittle upper crust and the brittle upper mantle prevents the syn-orogenic formation of a ductile crustal layer beneath the sedimentary cover. Arrival of the necking and proximal domains of the rifted margin (in which the ductile crust is preserved) at the subduction zone allows for the reactivation of the ductile middle crust as a décollement level. This triggers the switch to thick-skinned tectonics. Activation of this second and deeper décollement causes the re-deformation of the former thin-skinned décollement. Eventually, the mid-crustal décollement links to the main subduction interface, promoting underplating, crustal stacking, and exhumation of (metamorphic) units from the interior of the belt.

Acknowledgments

We thank O. Lacombe, L. Jolivet and two Anonymous Reviewers, as well as the Associate Editor, for their useful comments and suggestions. This is a contribution of the Institut de Recerca Geomodels from the Universitat de Barcelona.

FIGURE CAPTIONS

Figure 1. Scheme showing forward décollement propagation for (A) layer-cake lithosphere, and (B) magma-poor rifted margins. Rheological (strength) profiles are after Lescoutre and Manatschal (2020).

Figure 2. Geology of the Lurestan Arc area. (A) Simplified geological map of the study area, with inset showing the broader structural context of Zagros. (B) Schematic stratigraphy of the rocks involved in the Zagros orogeny. (C) Crustal section across the Lurestan Arc area (modified after Tavani et al, 2020, and Vergés et al., 2011; Moho depth after Jiménez-Munt et al., 2012; located in A). (D) Schematic representation of the Arabian rifted margin during Late Cretaceous (after Wrobel-Daveau et al., 2010).

Figure 3. (A) Geological cross-section across the inner part of the simply folded Lurestan belt (see Fig. 2A for location) with stratigraphic succession exposed in the area. (B) Thin-section of the base of the Garau Fm., showing a radiolarian packstone (35.04912°N; 46.16426°E). (C) Field photo illustrating exposure of the Garau Fm in the northeasternmost sector of the study area, with thick intervals of radiolarites (35.10778°N; 46.20355°E).

Figure 4. Geology of the southern Apennines. (A) Simplified geological map of the study area (modified after Ascione et al., 2012), with inset showing the structural framework of Italy. (B) Schematic stratigraphy of the different paleogeographic domains of Adria. (C) Crustal cross-section across the southern Apennines (modified after Mazzoli et al., 2014; location in A). The depth and thickness of the middle crust is speculative. (D) Schematic representation of the Adria rifted margin during Late Cretaceous.

Figure 5. Geological framework of the Oman mountains. (A) Simplified geological map of the Al-Hajar mountains, showing trace of geological section (modified after Corradetti et al., 2020). (B) Schematic stratigraphy of the rocks involved in the Oman orogeny. (C) Crustal cross-section across Jabal Akhdar. The depth and thickness of the middle crust is speculative. (D) Schematic representation of the Arabian rifted margin prior to the onset of convergence during Late Cretaceous times. MU (Musandam), JA (Jabal Akhdar) and SH (Saih Hatat) are the three main tectonic windows exposing the Arabian Platform domain.

Figure 6. Geology of the Taiwan Belt. (A) Simplified geological map of the Taiwan belt. (B) Schematic stratigraphy of the area. (C) Crustal cross-section (modified after Brown et al., 2012; location in A). The depth and thickness of the middle crust and mid-crustal stacking in the interior of the belt are speculative. (D) Schematic representation of the Eurasian rifted margin during Miocene times.

Figure 7. Schematic drawings of the evolutionary scenario by which a rifted continental margin becomes progressively involved in the deformation above a foreland-propagating, branching basal décollement. (A) Onset of shortening and localization of the deformation along a basal décollement confined within the sedimentary cover of the margin’s hyperextend domain (i.e., deep-water facies). (B) Bifurcation of the basal décollement, and involvement in the deformation of the sedimentary

cover of the margin’s necking domain (i.e., shallow water to slope sediments) at multiple structural levels. (C) Onset of inversion of pre-existing extensional faults located at the margin’s necking domain and basement-involved deformation. (D) Foreland- and deep-ward propagation of the basal décollement into mid-crustal structural levels of the margin’s necking to proximal domains, coeval with inception of high-pressure metamorphism and re-thickening of the ductile layer in the interior of the belt. (E) Progressive shortening above a mid-crustal décollement, with development of the basement ramps in the foreland part of the developing mountain belt and junction of the mid-crustal décollement with the subduction interface. (F) Final stage of the belt evolution, with basal accretion, nappe stacking and exhumation of the metamorphic units in the interior of the belt.

REFERENCES CITED

Ascione, A., Ciarcia, S., Di Donato, V., Mazzoli, S., and Vitale, S., 2012, The Pliocene-Quaternary wedge-top basins of southern Italy: an expression of propagating lateral slab tear beneath the Apennines: Basin Research, v. 24, p. 456–474, doi:10.1111/j.1365-2117.2011.00534.x.

Ballato, P., Uba, C.E., Landgraf, A., Strecker, M.R., Sudo, M., Stockli, D.F., Friedrich, A., and Tabatabaei, S.H., 2011, Arabia-Eurasia continental collision: Insights from late Tertiary foreland-basin evolution in the Alborz Mountains, northern Iran: Geological Society of America Bulletin, v. 123, p. 106–131, doi:10.1130/B30091.1.

Barber, D.E., Stockli, D.F., Horton, B.K., and Koshnaw, R.I., 2018, Cenozoic Exhumation and Foreland Basin Evolution of the Zagros Orogen During the Arabia-Eurasia Collision, Western Iran: Tectonics, v. 37, p. 4396–4420, doi:10.1029/2018TC005328.

Barrier, E., and Vrielynck, B., 2008, Palaeotectonic map of the Middle East, Atlas of 14 maps, tectonosedimentary-palinspastic maps from Late Norian to Pliocene: Commission for the Geologic Map of the World (CCMW, CCGM), Paris, France,.

Béchennec, F., Le Métour, J., Rabu, D., Villey, M., and Beurrier, M., 1988, The Hawasina Basin: A fragment of a starved passive continental margin, thrust over the Arabian Platform during obduction of the Sumail Nappe: Tectonophysics, v. 151, p. 323-343. doi:10.1016/0040-1951(88)90251-X.

Bellahsen, N., Jolivet, L., Lacombe, O., Bellanger, M., Boutoux, A., Garcia, S., Mouthereau, F., Le Pourhiet, L., and Gumiaux, C., 2012, Mechanisms of margin inversion in the external Western Alps: Implications for crustal rheology: Tectonophysics, v. 560–561, p. 62–83, doi:10.1016/j.tecto.2012.06.022.

Berberian, M., and King, G.C.P., 1981, Towards a paleogeography and tectonic evolution of Iran: Canadian Journal of Earth Sciences, v. 18, p. 210–265, doi:10.1139/e81-019.

Beyssac, O., Simoes, M., Avouac, J.P., Farley, K.A., Chen, Y.-G., Chan, Y.-C., and Goffé, B., 2007, Late Cenozoic metamorphic evolution and exhumation of Taiwan: Tectonics, v. 26, doi:10.1029/2006TC002064.

Boote, D.R.D., Mou, D., and Waite, R.I., 1990, Structural evolution of the Suneinah Foreland, Central Oman Mountains: Geological Society, London, Special Publications, v. 49, p. 397–418, doi:10.1144/GSL.SP.1992.049.01.25.

Breton, J.P., Béchennec, F., Le Métour, J., Moen-Maurel, L., and Razin, P., 2004, Eoalpine (Cretaceous) evolution of the Oman Tethyan continental margin: Insights from a structural field study in Jabal Akhdar (Oman Mountains): GeoArabia, v. 9, p. 41–58.

Brown, D., Alvarez-Marron, J., Schimmel, M., Wu, Y.-M., and Camanni, G., 2012, The structure and kinematics of the central Taiwan mountain belt derived from geological and seismicity data: Tectonics, v. 31, doi:10.1029/2012TC003156.

Brown, D., Alvarez-Marron, J., Biete, C., Kuo-Chen, H, Camanni, G., Ho, C.-W., 2017, How the structural architecture of the Eurasian continental margin affects the structure, seismicity, and topography of the south-central Taiwan fold and thrust belt. Tectonics, doi:10.1002/2017TC004475.

Butler, R.W.H., and Mazzoli, S., 2006, Styles of continental contraction: A review and introduction, *in* Styles of Continental Contraction, Geological Society of America, v. 80301, p. 1–10, doi:10.1130/2006.2414(01).

Byrne, T., Chan, Y.C., Rau, R.J., Lu, C.Y., Lee, Y.H., and Wang, Y.J., 2011, The Arc–Continent Collision in Taiwan, *in* Brown, D. and Ryan, P.D. eds., Arc-Continent Collision, Berlin, Heidelberg, Springer Berlin Heidelberg, p. 213–245.

Carrera, N., Muñoz, J.A., Sàbat, F., Mon, R., and Roca, E., 2006, The role of inversion tectonics in the structure of the Cordillera Oriental (NW Argentinean Andes): Journal of Structural Geology, v. 28, p. 1921–1932, doi:10.1016/j.jsg.2006.07.006.

Chenin, P., Manatschal, G., Picazo, S., Müntener, O., Karner, G., Johnson, C., & Ulrich, M., 2017, Influence of the architecture of magma-poor hyperextended rifted margins on orogens produced by the closure of narrow versus wide oceans. Geosphere, v. 13, p. 559-576, doi:10.1130/GES01363.1

Chemenda, A.I., Mattauer, M., and Bokun, A.N., 1996, Continental subduction and a mechanism for exhumation of high-pressure metamorphic rocks: new modelling and field data from Oman: Earth and Planetary Science Letters, v. 143, p. 173–182, doi:10.1016/0012-821X(96)00123-9.

Chen, W.-S., Chung, S.-L., Chou, H.-Y., Zugeerbai, Z., Shao, W.-Y., and Lee, Y.-H., 2017, A reinterpretation of the metamorphic Yuli belt: Evidence for a middle-late Miocene accretionary prism in eastern Taiwan: Tectonics, v. 36, p. 188–206, doi:10.1002/2016TC004383.

Clark, M.B., Fisher, D.M., Lu, C.-Y., and Chen, C.-H., 1993, Kinematic analyses of the Hsüehshan Range, Taiwan: A large-scale pop-up structure: Tectonics, v. 12, p. 205–217, doi:10.1029/92TC01711.

Cohen, C.R., 1982, Model for a passive to active continental margin transition: implications for hydrocarbon exploration.: American Association of Petroleum Geologists Bulletin, v. 66, p. 708–718, doi:10.1306/03b5b6f5-16d1-11d7-8645000102c1865d.

Cooper, D.J.W., 1988, Structure and sequence of thrusting in deep-water sediments during ophiolite emplacement in the south-central Oman Mountains: Journal of Structural Geology, v. 10, p. 473–485, doi:10.1016/0191-8141(88)90035-1.

Cooper, D.J.W., Ali, M.Y., and Searle, M.P., 2014, Structure of the northern Oman Mountains from the Semail Ophiolite to the Foreland Basin: Geological Society, London, Special Publications, v. 392, p. 129–153, doi:10.1144/SP392.7.

Cooper, M.A., Williams, G.D., de Graciansky, P.C., Murphy, R.W., Needham, T., de Paor, D., Stoneley, R., Todd, S.P., Turner, J.P., and Ziegler, P.A., 1989, Inversion tectonics — a discussion: Geological Society, London, Special Publications, v. 44, p. 335–347, doi:10.1144/GSL.SP.1989.044.01.18.

Corradetti, A., Spina, V., Tavani, S., Ringenbach, J.C., Sabbatino, M., Razin, P., Laurent, O., Brichau, S., and Mazzoli, S., 2020, Late-stage tectonic evolution of the Al-Hajar Mountains, Oman: new constraints from Palaeogene sedimentary units and low-temperature thermochronometry: Geological Magazine, v. 157, p. 1031-1044, doi:10.1017/S0016756819001250.

Cosentino, D., Cipollari, P., Marsili, P., and Scrocca, D., 2010, Geology of the central Apennines: a regional review: Journal of the Virtual Explorer, v. 36.

Curzi, M., Billi, A., Carminati, E., Rossetti, F., Albert, R., Aldega, L., Cardello, L., Conti, A., Gerdes, A., Smeraglia, L., Van der Lelij, R., Vignaroli, G., & Viola, G. (2020). Disproving the presence of Paleozoic-Triassic metamorphic rocks on the Island of Zannone (central Italy): Implications for the early stages of the Tyrrhenian-Apennines tectonic evolution. Tectonics, e2020TC006296.

D'Argenio, B., Pescatore, T., and Scandone, P., 1975, Structural pattern of the Campania-Lucania Apennines, *in* Structural Model of Italy, Quaderni Ricerca Scientifica CNR, v. 90, p. 313–327.

De Wever, P., Azema, J., and Fourcade, E., 1994, Radiolaires et radiolarites : production primaire, diagenèse et paléogéographie; Radiolarians and radiolarites : primary production, diagenesis and paleogeography: Bulletin des centres de recherches exploration - Production Elf-Aquitaine, v. 18, p. 315–379.

Dewey, J.F., Helman, M.L., Knott, S.D., Turco, E., and Hutton, D.H.W., 1989, Kinematics of the western Mediterranean: Geological Society, London, Special Publications, v. 45, p. 265–283, doi:10.1144/GSL.SP.1989.045.01.15.

Di Bucci, D., Ravaglia, A., Seno, S., Toscani, G., Fracassi, U., and Valensise, G., 2006, Seismotectonics of the southern Apennines and Adriatic foreland: Insights on active regional E-W shear zones from analogue modeling: Tectonics, v. 25, doi:10.1029/2005TC001898.

Doglioni, C., 1991, A proposal for the kinematic modelling of W-dipping subductions - possible applications to the Tyrrhenian-Apennines system: Terra Nova, v. 3, p. 423–434, doi:10.1111/j.1365-3121.1991.tb00172.x.

Dorsey, R.J., 1988, Provenance Evolution and Unroofing History of a Modern Arc-Continent Collision: Evidence from Petrography of Plio-pleistocene Sandstones, Eastern Taiwan: SEPM Journal of Sedimentary Research, v. Vol. 58, doi:10.1306/212F8D5A-2B24-11D7-8648000102C1865D.

Faccenna, C. et al., 2014, Mantle dynamics in the Mediterranean: Reviews of Geophysics, v. 52, p.

283–332, doi:10.1002/2013RG000444.

Gharib, F., and De Wever, P., 2010, Radiolaires mésozoïques de la formation de Kermanshah (Iran): Comptes Rendus Palevol, v. 9, p. 209–219, doi:10.1016/j.crpv.2010.06.003.

Ghasemi, A., and Talbot, C.J., 2006, A new tectonic scenario for the Sanandaj–Sirjan Zone (Iran): Journal of Asian Earth Sciences, v. 26, p. 683–693, doi:10.1016/j.jseaes.2005.01.003.

Glennie, K.W., and Boegner, P.L., 1981, Sole pit inversion tectonics, *in* Illing, L. V. and D., H.G. eds., Petroleum Geology of the Continental Shelf of North-West Europe., London, p. 110–120.

Glennie, K.W., Boeuf, M.G.A., Clarke, M.W.H., Moody-Stuart, M., Pilaar, W.F.H., and Reinhardt, B.M., 1973, Late Cretaceous nappes in Oman Mountains and their geologic evolution: AAPG Bulletin, v. 57, p. 5–27.

Gourley, J.R., Byrne, T., Chan, Y.-C., Wu, F., and Rau, R.-J., 2007, Fault geometries illuminated from seismicity in central Taiwan: Implications for crustal scale structural boundaries in the northern Central Range: Tectonophysics, v. 445, p. 168–185, doi:10.1016/j.tecto.2007.08.013.

Granado, P., and Ruh, J.B., 2019, Numerical modelling of inversion tectonics in fold-and-thrust belts: Tectonophysics, v. 763, p. 14–29, doi:10.1016/j.tecto.2019.04.033.

Grobe, A., Virgo, S., von Hagke, C., Urai, J.L., and Littke, R., 2018, Multiphase Structural Evolution of a Continental Margin During Obduction Orogeny: Insights From the Jebel Akhdar Dome, Oman Mountains: Tectonics, v. 37, p. 888–913, doi:10.1002/2016TC004442.

Hacker, B.R., 1994, Rapid emplacement of young oceanic lithosphere: Argon geochronology of the oman ophiolite: Science, v. 265, p. 1563–1565, doi:10.1126/science.265.5178.1563.

Handy, M.R., M. Schmid, S., Bousquet, R., Kissling, E., and Bernoulli, D., 2010, Reconciling plate-tectonic reconstructions of Alpine Tethys with the geological–geophysical record of spreading and subduction in the Alps: Earth-Science Reviews, v. 102, p. 121–158, doi:10.1016/j.earscirev.2010.06.002.

Hansman, R.J., Albert, R., Gerdes, A., and Ring, U., 2018, Absolute ages of multiple generations of brittle structures by U-Pb dating of calcite: Geology, v. 46, p. 207–210.

Hansman, R.J., Ring, U., Thomson, S.N., den Brok, B., and Stübner, K., 2017, Late Eocene Uplift of the Al Hajar Mountains, Oman, Supported by Stratigraphy and Low-Temperature Thermochronology: Tectonics, v. 36, p. 3081–3109, doi:10.1002/2017TC004672.

Hessami, K., Koyi, H.A., and Talbot, C.J., 2001, The significance of strike-slip faulting in the basement of the Zagros fold and thrust belt: Journal of Petroleum Geology, v. 24, p. 5–28, doi:10.1111/j.1747-5457.2001.tb00659.x.

Homewood, P., Allen, P.A., and Williams, G.D., 1986, Dynamics of the Molasse Basin of Western Switzerland, *in* Foreland Basins, Oxford, UK, Blackwell Publishing Ltd., p. 199–217, doi:10.1002/9781444303810.ch10.

Homke, S., Vergés, J., Serra-Kiel, J., Bernaola, G., Sharp, I., Garcés, M., Montero-Verdú, I., Karpuz, R., and Goodarzi, M.H., 2009, Late Cretaceous–Paleocene formation of the proto–Zagros foreland basin, Lurestan Province, SW Iran: GSA Bulletin, v. 121, p. 963–978, doi:10.1130/B26035.1.

Huang, C.-Y., Yuan, P.B., and Tsao, S.-J., 2006, Temporal and spatial records of active arc-continent collision in Taiwan: A synthesis: Geological Society of America Bulletin, v. 118, p. 274–288, doi:10.1130/B25527.1.

ISPRA, 2011, Carta geologica d'Italia, Isola di Capri (Foglio 484): Servizio Geologico d'Italia, scale 1:25,000, sheet 484.

Jackson, J.A., 1980, Reactivation of basement faults and crustal shortening in orogenic belts: Nature, v. 283, p. 343–346, doi:10.1038/283343a0.

Jacobs, J., Thomas, R.J., Ksienzyk, A.K., and Dunkl, I., 2015, Tracking the Oman Ophiolite to the surface - New fission track and (U-Th)/He data from the Aswad and Khor Fakkan Blocks, United Arab Emirates: Tectonophysics, v. 644, p. 68–80, doi:10.1016/j.tecto.2014.12.018.

Jamieson, R.A., and Beaumont, C., 2013, On the origin of orogens: Geological Society of America Bulletin, v. 125, p. 1671–1702, doi:10.1130/B30855.1.

Jammes, S., Huismans, R.S., and Muñoz, J.A., 2014, Lateral variation in structural style of mountain building: Controls of rheological and rift inheritance: Terra Nova, v. 26, p. 201–207, doi:10.1111/ter.12087.

Jassim, S.Z., and Goff, J.C., 2006, Geology of Iraq (S. Z. Jassim & J. C. Goff, Eds.): Dolin, Prague and Moravian Museum, Brno, 341 p.

Jiménez-Munt, I., Fernàndez, M., Saura, E., Vergés, J., and Garcia-Castellanos, D., 2012, 3-D lithospheric structure and regional/residual Bouguer anomalies in the Arabia-Eurasia collision (Iran): Geophysical Journal International, v. 190, p. 1311–1324, doi:10.1111/j.1365-246X.2012.05580.x.

Jolivet, L., Faccenna, C., Agard, P., Frizon de Lamotte, D., Menant, A., Sternai, P., Guillocheau, F., and Polat, A., 2016, Neo-Tethys geodynamics and mantle convection: from extension to compression in Africa and a conceptual model for obduction 1: Canadian Journal of Earth Sciences, v. 53, p. 1190–1204, doi:10.1139/cjes-2015-0118.

Keyser, W., Tsai, C.-H., Iizuka, Y., Oberhänsli, R., and Ernst, W.G., 2016, High-pressure metamorphism in the Chinshuichi area, Yuli belt, eastern Taiwan: Tectonophysics, v. 692, p. 191–202, doi:10.1016/j.tecto.2015.09.012.

Knott, S.D., 1987, The Liguride Complex of Southern Italy — a Cretaceous to Paleogene accretionary wedge: Tectonophysics, v. 142, p. 217–226, doi:10.1016/0040-1951(87)90124-7.

Koshnaw, R.I., Horton, B.K., Stockli, D.F., Barber, D.E., Tamar-Agha, M.Y., and Kendall, J.J., 2017, Neogene shortening and exhumation of the Zagros fold-thrust belt and foreland basin in the Kurdistan region of northern Iraq: Tectonophysics, v. 694, p. 332–355, doi:10.1016/j.tecto.2016.11.016.

Kuo-Chen, H., Wu, F.T., and Roecker, S.W., 2012, Three-dimensional P velocity structures of the lithosphere beneath Taiwan from the analysis of TAIGER and related seismic data sets: Journal of Geophysical Research: Solid Earth, v. 117, doi:10.1029/2011JB009108.

Lacombe, O., and Bellahsen, N., 2016, Thick-skinned tectonics and basement-involved fold–thrust belts: insights from selected Cenozoic orogens: Geological Magazine, v. 153, p. 763–810, doi:10.1017/S0016756816000078.

Lacombe, O., and Mouthereau, F., 2002, Basement-involved shortening and deep detachment tectonics in forelands of orogens: Insights from recent collision belts (Taiwan, Western Alps, Pyrenees): Tectonics, v. 21, p. 12-1-12–22, doi:10.1029/2001TC901018.

Lacombe, O., Mouthereau, F., Deffontaines, B., Angelier, J., Chu, H.T., and Lee, C.T., 1999, Geometry and Quaternary kinematics of fold-and-thrust units of southwestern Taiwan: Tectonics, v. 18, p. 1198–1223, doi:10.1029/1999TC900036.

Lavier, L.L., and Manatschal, G., 2006, A mechanism to thin the continental lithosphere at magma-poor margins: Nature, v. 440, p. 324–328, doi:10.1038/nature04608.

Lee, Y.-H., Chen, C.-C., Liu, T.-K., Ho, H.-C., Lu, H.-Y., and Lo, W., 2006, Mountain building mechanisms in the Southern Central Range of the Taiwan Orogenic Belt — From accretionary wedge deformation to arc–continental collision: Earth and Planetary Science Letters, v. 252, p. 413–422, doi:10.1016/j.epsl.2006.09.047.

Lescoutre, R., and Manatschal, G., 2020, Role of rift-inheritance and segmentation for orogenic evolution: example from the Pyrenean-Cantabrian system: Bulletin de la Société Géologique de France, v. In Press.

Lin, A.T., Watts, A.B., and Hesselbo, S.P., 2003, Cenozoic stratigraphy and subsidence history of the South China Sea margin in the Taiwan region: Basin Research, v. 15, p. 453–478, doi:10.1046/j.1365-2117.2003.00215.x.

Lister, G.S., Etheridge, M.A., and Symonds, P.A., 1986, Detachment faulting and the evolution of passive continental margins: Geology, v. 14, p. 246, doi:10.1130/0091-7613(1986)14<246:DFATEO>2.0.CO;2.

Macedo, J., and Marshak, S., 1999, Controls on the geometry of fold-thrust belt salients: Geological Society of America Bulletin, v. 111, p. 1808–1822, doi:10.1130/0016-7606(1999)111<1808:COTGOF>2.3.CO;2.

MacKay, M.E., 1995, Structural variation and landward vergence at the toe of the Oregon accretionary prism: Tectonics, v. 14, p. 1309–1320, doi:10.1029/95TC02320.

Marshak, S., Karlstom, K., and Timmons, J.M., 2000, Inversion of proterozoic extensional faults: An explanation for the pattern of Laramide and Ancestral rockies intracratonic deformation, United States: Geology, v. 28, p. 735–738, doi:10.1130/0091-

7613(2000)28<735:IOPEFA>2.0.CO;2.

Mazzoli, S., Ascione, A., Buscher, J.T., Pignalosa, A., Valente, E., and Zattin, M., 2014, Low-angle normal faulting and focused exhumation associated with late Pliocene change in tectonic style in the southern Apennines (Italy): Tectonics, v. 33, p. 1802–1818, doi:10.1002/2014TC003608.

Mazzoli, S., Barkham, S., Cello, G., Gambini, R., Mattioni, L., Shiner, P., and Tondi, E., 2001, Reconstruction of continental margin architecture deformed by the contraction of the Lagonegro Basin, southern Apennines, Italy: Journal of the Geological Society, v. 158, p. 309–319.

McIntosh, K., van Avendonk, H., Lavier, L., Lester, W.R., Eakin, D., Wu, F., Liu, C.-S., and Lee, C.-S., 2013, Inversion of a hyper-extended rifted margin in the southern Central Range of Taiwan: Geology, v. 41, p. 871–874, doi:10.1130/G34402.1.

McIntosh, K., Nakamura, Y., Wang, T.-K., Shih, R.-C., Chen, A., and Liu, C.-S., 2005, Crustal-scale seismic profiles across Taiwan and the western Philippine Sea: Tectonophysics, v. 401, p. 23–54, doi:10.1016/j.tecto.2005.02.015.

Menardi Noguera, A., and Rea, G., 2000, Deep structure of the Campanian–Lucanian Arc (Southern Apennine, Italy): Tectonophysics, v. 324, p. 239–265, doi:10.1016/S0040-1951(00)00137-2.

Mohn, G., Manatschal, G., Beltrando, M., Masini, E., and Kusznir, N., 2012, Necking of continental crust in magma-poor rifted margins: Evidence from the fossil Alpine Tethys margins: Tectonics, v. 31, doi:10.1029/2011TC002961.

Molli, G., and Malavieille, J., 2011, Orogenic processes and the Corsica/Apennines geodynamic evolution: insights from Taiwan: International Journal of Earth Sciences, v. 100, p. 1207–1224, doi:10.1007/s00531-010-0598-y.

Moore, G.F., Shipley, T.H., Stoffa, P.L., Karig, D.E., Taira, A., Kuramoto, S., Tokuyama, H., and Suyehiro, K., 1990, Structure of the Nankai Trough Accretionary Zone from multichannel seismic reflection data: Journal of Geophysical Research, v. 95, p. 8753, doi:10.1029/JB095iB06p08753.

Mount, V.S., Crawford, R.I.S., and Bergman, S.C., 1998, Regional structural style of the Central and Southern Oman Mountains: Jebel Akhdar, Saih Hatat, and the Northern Ghaba Basin: GeoArabia, v. 3, p. 475–490.

Mouthereau, F., Deffontaines, B., Lacombe, O., and Angelier, J., 2002, Variations along the strike of the Taiwan thrust belt: Basement control on structural style, wedge geometry, and kinematics, *in* Byrne, T.B. and Liu, C.-S. eds., Geology and Geophysics of an Arc-continent Collision, Taiwan, Republic of China, Colorado, Boulder, p. 35–58.

Mouthereau, F., and Lacombe, O., 2006, Inversion of the Paleogene Chinese continental margin and thick-skinned deformation in the Western Foreland of Taiwan: Journal of Structural Geology, v. 28, p. 1977–1993, doi:10.1016/j.jsg.2006.08.007.

Mouthereau, F., Lacombe, O., and Vergés, J., 2012, Building the Zagros collisional orogen: Timing, strain distribution and the dynamics of Arabia/Eurasia plate convergence: Tectonophysics, v. 532–535, p. 27–60, doi:10.1016/j.tecto.2012.01.022.

Muñoz, J.A., Beamud, E., Fernández, O., Arbués, P., Dinarès-Turell, J., and Poblet, J., 2013, The Ainsa Fold and thrust oblique zone of the central Pyrenees: Kinematics of a curved contractional system from paleomagnetic and structural data: Tectonics, v. 32, p. 1–34, doi:10.1002/tect.20070.

Nemcok, M., Gayer, R., and Miliorizos, M., 1995, Structural analysis of the inverted Bristol Channel Basin: implications for the geometry and timing of fracture porosity: Geological Society, London, Special Publications, v. 88, p. 355–392, doi:10.1144/GSL.SP.1995.088.01.20.

Nemčok, M., Mora, A., and Cosgrove, J., 2013, Thick-skin-dominated orogens; from initial inversion to full accretion: An introduction: Geological Society Special Publication, v. 377, p. 1–17, doi:10.1144/SP377.17.

Ogniben, L., 1969, Schema introduttivo alla geologia del confine calabro-lucano: Mem. Soc. Geol. It., v. 8, p. 453–763.

Oncken, O., von Winterfeld, C., and Dittmar, U., 1999, Accretion of a rifted passive margin: The

Late Paleozoic Rhenohercynian fold and thrust belt (Middle European Variscides): Tectonics, v. 18, p. 75–91, doi:10.1029/98TC02763.

Patacca, E., and Scandone, P., 2007, Geology of the southern Apennines: Bollettino della Società Geologica Italiana, v. 7, p. 75–119.

Péron-Pinvidic, G., and Manatschal, G., 2009, The final rifting evolution at deep magma-poor passive margins from Iberia-Newfoundland: a new point of view: International Journal of Earth Sciences, v. 98, p. 1581–1597, doi:10.1007/s00531-008-0337-9.

Péron-Pinvidic, G., & Manatschal, G., 2010, From microcontinents to extensional allochthons: witnesses of how continents rift and break apart?. Petroleum Geoscience, v. 16, p. 189-197. doi:10.1144/1354-079309-903

Pfiffner, O.A., 2017, Thick-Skinned and Thin-Skinned Tectonics: A Global Perspective: Geosciences, v. 7, p. 71, doi:10.3390/geosciences7030071.

Rabu, D. et al., 1993, Stratigraphy and structure of the Oman mountains: Documents - BRGM, 300 p.

Rioux, M., Bowring, S., Kelemen, P., Gordon, S., Dudás, F., and Miller, R., 2012, Rapid crustal accretion and magma assimilation in the Oman-U.A.E. ophiolite: High precision U-Pb zircon geochronology of the gabbroic crust: Journal of Geophysical Research: Solid Earth, v. 117, p. 1–12, doi:10.1029/2012JB009273.

Robertson, A.H.F., and Searle, M.P., 1990, The northern Oman Tethyan continental margin: stratigraphy, structure, concepts and controversies: Geological Society, London, Special Publications, v. 49, p. 3–25, doi:10.1144/GSL.SP.1992.049.01.02.

Roure, F., Casero, P., and Vially, R., 1991, Growth processes and melange formation in the southern Apennines accretionary wedge: Earth and Planetary Science Letters, v. 102, p. 395–412.

Saddiqi, O., Michard, A., Goffe, B., Poupeau, G., and Oberhänsli, R., 2006, Fission-track thermochronology of the Oman Mountains continental windows, and current problems of tectonic interpretation: Bulletin de la Societe Geologique de France, v. 177, p. 127–143, doi:10.2113/gssgfbull.177.3.127.

Santantonio, M., and Carminati, E., 2011, Jurassic rifting evolution of the Apennines and Southern Alps (Italy): Parallels and differences: Geological Society of America Bulletin, v. 123, p. 468–484, doi:10.1130/B30104.1.

Saura, E., Garcia-Castellanos, D., Casciello, E., Parravano, V., Urruela, A., and Vergés, J., 2015, Modeling the flexural evolution of the Amiran and Mesopotamian foreland basins of NW Zagros (Iran-Iraq): Tectonics, v. 34, p. 377–395, doi:10.1002/2014TC003660.

Schmid, S.M., Fügenschuh, B., Kissling, E., and Schuster, R., 2004, Tectonic map and overall architecture of the Alpine orogen: Eclogae Geologicae Helvetiae, v. 97, p. 93–117, doi:10.1007/s00015-004-1113-x.

Schmid, S.M., and Kissling, E., 2000, The arc of the western Alps in the light of geophysical data on deep crustal structure: Tectonics, v. 19, p. 62–85, doi:10.1029/1999TC900057.

Scrocca, D., Carminati, E., and Doglioni, C., 2005. Deep structure of the southern Apennines, Italy: Thin-skinned or thick-skinned?. Tectonics, v. 24, TC3005, doi:10.1029/2004TC001634

Scrocca, D., 2010, Southern Apennines: structural setting and tectonic evolution: Journal of the Virtual Explorer, v. 36, doi:10.3809/jvirtex.2010.00225.

Searle, M.P., and Cox, J., 2002, Subduction zone metamorphism during formation and emplacement of the Semail ophiolite in the Oman Mountains: Geological Magazine, v. 139, p. 241–255, doi:10.1017/S0016756802006532.

Shyu, J.B.H., Sieh, K., Chen, Y.-G., Chuang, R.Y., Wang, Y., and Chung, L.-H., 2008, Geomorphology of the southernmost Longitudinal Valley fault: Implications for evolution of the active suture of eastern Taiwan: Tectonics, v. 27, doi:10.1029/2006TC002060.

Sibuet, J.-C., and Hsu, S.-K., 2004, How was Taiwan created? Tectonophysics, v. 379, p. 159–181, doi:10.1016/j.tecto.2003.10.022.

Simoes, M., Avouac, J.P., Beyssac, O., Goffé, B., Farley, K.A., and Chen, Y.-G., 2007, Mountain building in Taiwan: A thermokinematic model: Journal of Geophysical Research, v. 112, p. B11405, doi:10.1029/2006JB004824.

Simoes, M., Beyssac, O., and Chen, Y.-G., 2012, Late Cenozoic metamorphism and mountain building in Taiwan: A review: Journal of Asian Earth Sciences, v. 46, p. 92–119, doi:10.1016/j.jseaes.2011.11.009.

Somma, R., Messina, A., and Mazzoli, S., 2005, Syn-orogenic extension in the Peloritani Alpine Thrust Belt (NE Sicily, Italy): Evidence from the Alì Unit: Comptes Rendus Geoscience, v. 337, p. 861–871, doi:10.1016/j.crte.2005.03.004.

Sutra, E., Manatschal, G., Mohn, G., and Unternehr, P., 2013, Quantification and restoration of extensional deformation along the Western Iberia and Newfoundland rifted margins: Geochemistry, Geophysics, Geosystems, v. 14, p. 2575–2597, doi:10.1002/ggge.20135.

Talebian, M., and Jackson, J., 2004, A reappraisal of earthquake focal mechanisms and active shortening in the Zagros mountains of Iran: Geophysical Journal International, v. 156, p. 506–526, doi:10.1111/j.1365-246X.2004.02092.x.

Tang, C.-C., Zhu, L., Chen, C.-H., and Teng, T.-L., 2011, Significant crustal structural variation across the Chaochou Fault, southern Taiwan: New tectonic implications for convergent plate boundary: Journal of Asian Earth Sciences, v. 41, p. 564–570, doi:10.1016/j.jseaes.2010.12.003.

Tarapoanca, M., Andriessen, P., Broto, K., Chérel, L., Ellouz-Zimmermann, N., Faure, J.-L., Jardin, A., Naville, C., and Roure, F., 2010, Forward kinematic modelling of a regional transect in the Northern Emirates using geological and apatite fission track age constraints on paleo-burial history: Arabian Journal of Geosciences, v. 3, p. 395–411, doi:10.1007/s12517-010-0213-3.

Tavani, S., Camanni, G., Nappo, M., Snidero, M., Ascione, A., Valente, E., Gharabeigli, G., Morsalnejad, D., and Mazzoli, S., 2020, The Mountain Front Flexure in the Lurestan region of the Zagros belt: Crustal architecture and role of structural inheritances: Journal of Structural Geology, v. 135, p. 104022, doi:10.1016/j.jsg.2020.104022.

Tavani, S., Parente, M., Puzone, F., Corradetti, A., Gharabeigli, G., Valinejad, M., Morsalnejad, D., and Mazzoli, S., 2018a, The seismogenic fault system of the 2017 M w 7.3 Iran–Iraq earthquake: constraints from surface and subsurface data, cross-section balancing, and restoration: Solid Earth, v. 9, p. 821–831, doi:10.5194/se-9-821-2018.

Tavani, S., Parente, M., Vitale, S., Iannace, A., Corradetti, A., Bottini, C., Morsalnejad, D., and Mazzoli, S., 2018b, Early Jurassic Rifting of the Arabian Passive Continental Margin of the Neo-Tethys. Field Evidence From the Lurestan Region of the Zagros Fold-and-Thrust Belt, Iran: Tectonics, v. 37, p. 2586–2607, doi:10.1029/2018TC005192.

Teng, L.S., 1990, Geotectonic evolution of late Cenozoic arc-continent collision in Taiwan: Tectonophysics, v. 183, p. 57–76, doi:10.1016/0040-1951(90)90188-E.

Teng, L.S., and Lin, A.T., 2004, Cenozoic tectonics of the China continental margin: insights from Taiwan, *in* Malpas, J., Fletcher, C.J.N., Ali, J.R., and Aitchison, J.C. eds., Aspects of the Tectonic Evolution of China, Geological Society, London, Special Publications, 226, v. 226, p. 313–332, doi:10.1144/GSL.SP.2004.226.01.17.

Vergés, J., Saura, E., Casciello, E., Fernàndez, M., Villaseñor, A., Jiménez-Munt, I., and García-Castellanos, D., 2011, Crustal-scale cross-sections across the NW Zagros belt: implications for the Arabian margin reconstruction: Geological Magazine, v. 148, p. 739–761, doi:10.1017/S0016756811000331.

Warburton, J., Burnhill, T.J., Graham, R.H., and Isaac, K.P., 1990, The evolution of the Oman Mountains Foreland Basin, *in* Robertson, A.F.H., Searle, M.P., and Ries, A.C. eds., The Geology and Tectonics of the Oman Region. Geological Society of London, Special Publications, v. 49, p. 419–427, doi:10.1144/GSL.SP.1992.049.01.26.

Warren, C.J., Parrish, R.R., Searle, M.P., and Waters, D.J., 2003, Dating the subduction of the Arabian continental margin beneath the Semail ophiolite, Oman: Geology, v. 31, p. 889–892, doi:10.1130/G19666.1.

Whitmarsh, R.B., Manatschal, G., and Minshull, T.A., 2001, Evolution of magma-poor continental margins from rifting to seafloor spreading: Nature, v. 413, p. 150–154, doi:10.1038/35093085.

Williams, G.D., Powell, C.M., and Cooper, M.A., 1989, Geometry and kinematics of inversion tectonics: Geological Society, London, Special Publications, v. 44, p. 3–15, doi:10.1144/GSL.SP.1989.044.01.02.

Wilson, J.T., 1966, Did the Atlantic Close and then Re-Open? Nature, v. 211, p. 676–681, doi:10.1038/211676a0.

Wrobel-Daveau, J.-C., Ringenbach, J.-C., Tavakoli, S., Ruiz, G.M.H., Masse, P., and Frizon de Lamotte, D., 2010, Evidence for mantle exhumation along the Arabian margin in the Zagros (Kermanshah area, Iran): Arabian Journal of Geosciences, v. 3, p. 499–513, doi:10.1007/s12517-010-0209-z.

Wu, Y.-M., Chang, C.-H., Zhao, L., Shyu, J.B.H., Chen, Y.-G., Sieh, K., and Avouac, J.-P., 2007, Seismic tomography of Taiwan: Improved constraints from a dense network of strong motion stations: Journal of Geophysical Research, v. 112, p. B08312, doi:10.1029/2007JB004983.

Yue, L.-F., Suppe, J., and Hung, J.-H., 2005, Structural geology of a classic thrust belt earthquake: the 1999 Chi-Chi earthquake Taiwan (Mw=7.6): Journal of Structural Geology, v. 27, p. 2058–2083, doi:10.1016/j.jsg.2005.05.020.

Zanchi, A., Berra, F., Mattei, M., R. Ghassemi, M., and Sabouri, J., 2006, Inversion tectonics in central Alborz, Iran: Journal of Structural Geology, v. 28, p. 2023–2037, doi:10.1016/j.jsg.2006.06.020.

Figure 1

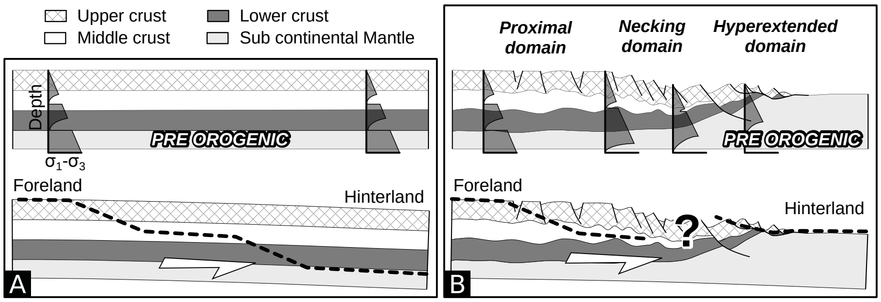

Figure 1
2 columns in 3 column layout

Figure 2

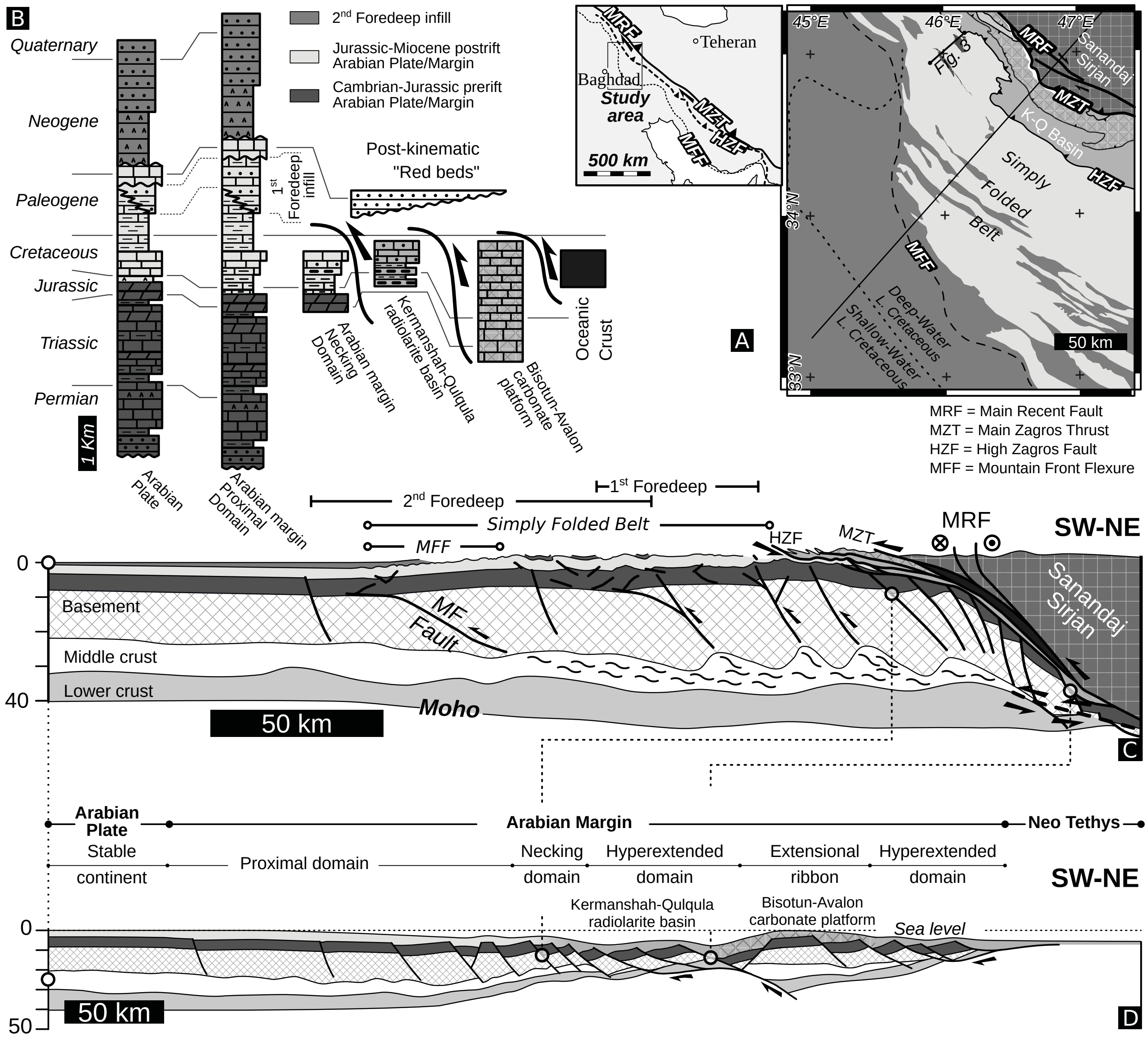

Figure 2
3 columns in 3 column layout

Figure 3

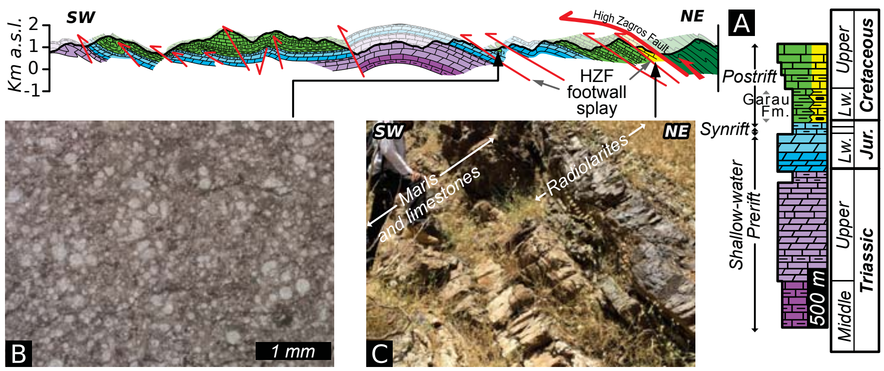

Figure 3
2 columns in 3 column layout

Figure 4

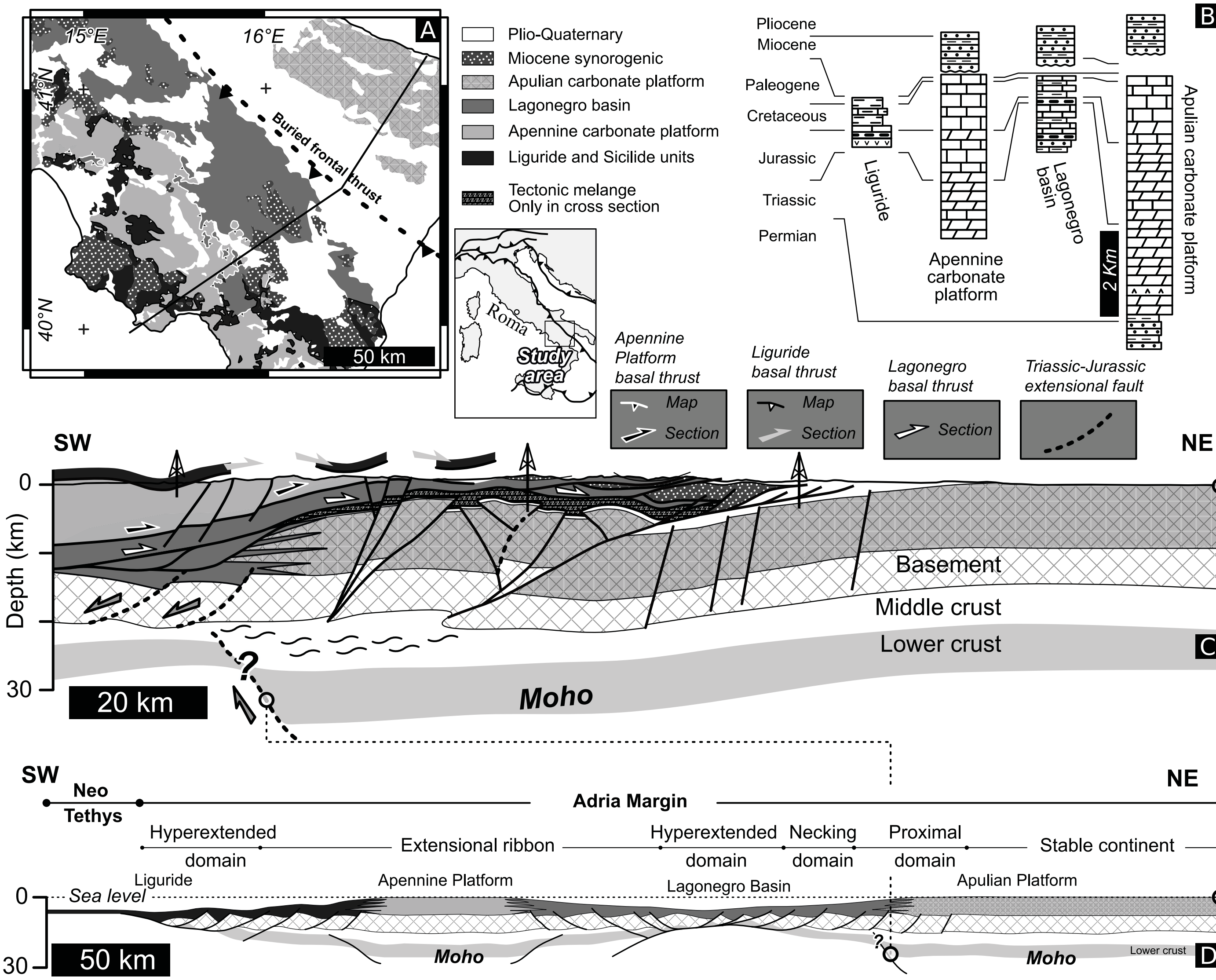

Figure 4
3 columns in 3 column layout

Figure 5

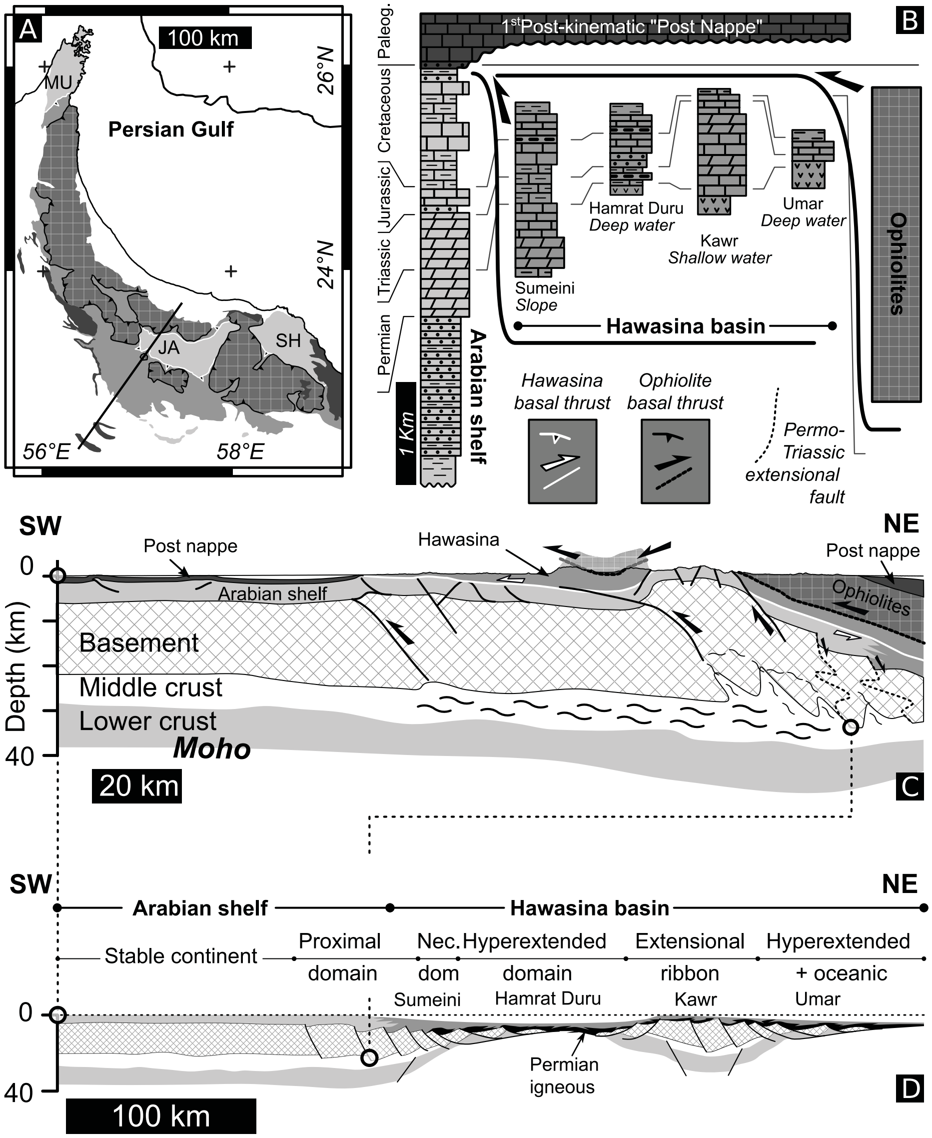

Figure 5
2 columns in 3 column layout

Figure 6

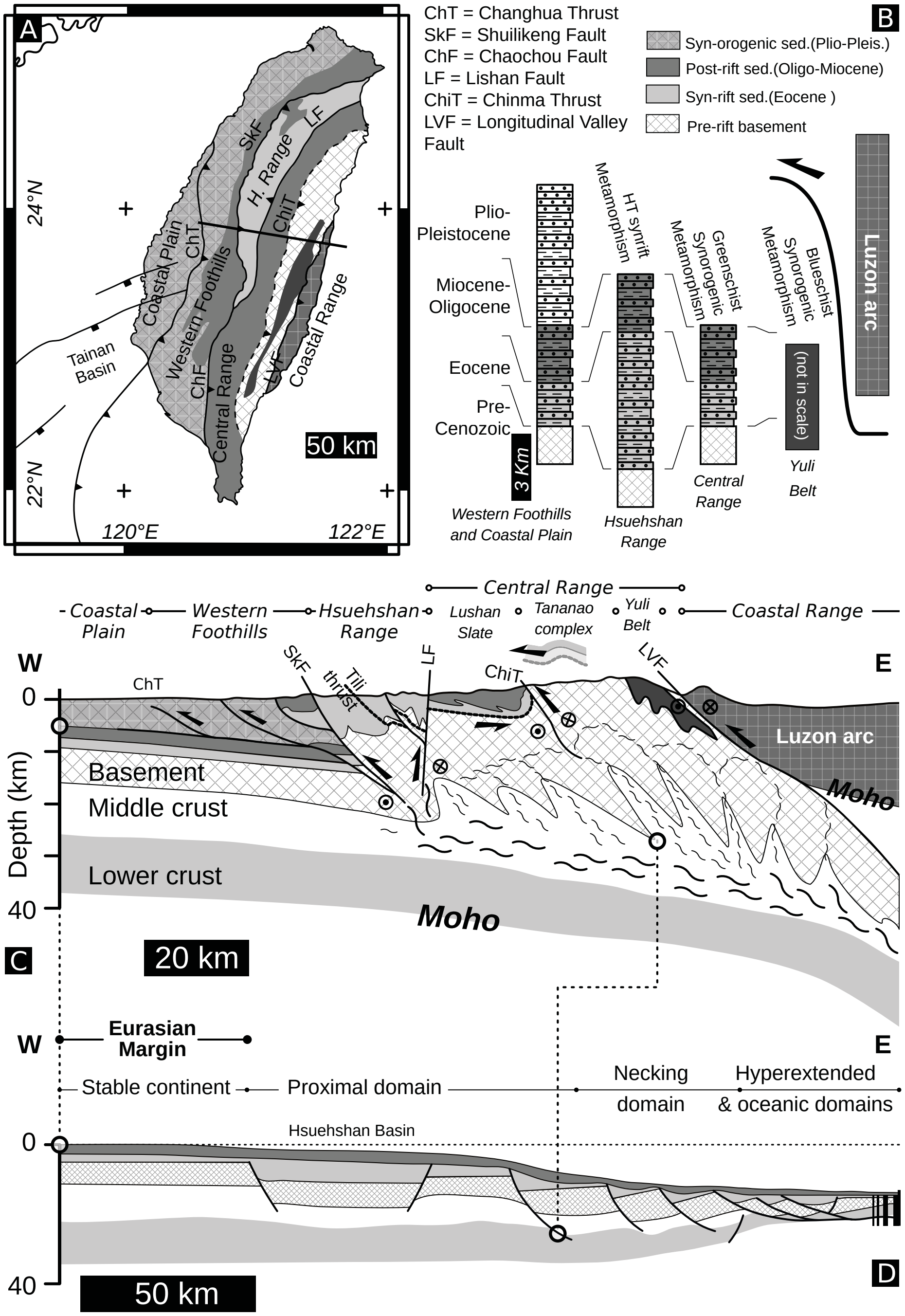

Figure 6
2 columns in 3 column layout

Figure 7

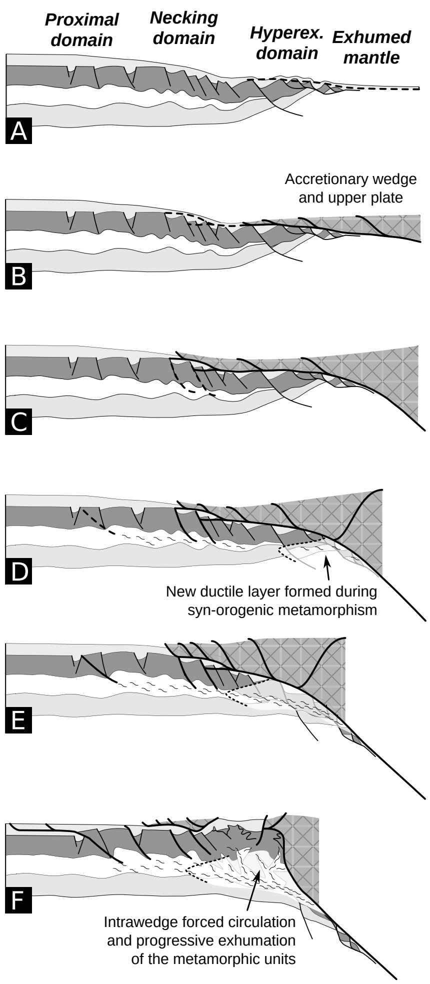

Figure 7
1 column in 3 column layout